CHALMERS

The Preview Curvature Controller for a Passenger Car Steering Robot

Development of a closed-loop path controller for repeatable vehicle dynamics testing

Master's Thesis in the Master's programme Automotive Engineering

KLAS OLSSON, CARL SANDBERG

Department of Applied Mechanics
Division of Vehicle Engineering and Autonomous Systems
CHALMERS UNIVERSITY OF TECHNOLOGY
Göteborg, Sweden 2011
Master's Thesis 2011:41

MASTER’S THESIS 2011:41

The Preview Curvature Controller for a Passenger Car Steering Robot

Development of a closed-loop path controller for repeatable vehicle dynamics testing

Master’s Thesis in the Master’s programme Automotive Engineering and Systems, Control and Mechatronics

KLAS OLSSON, CARL SANDBERG

Department of Applied Mechanics
Division of Vehicle Engineering and Autonomous Systems
CHALMERS UNIVERSITY OF TECHNOLOGY

Göteborg, Sweden 2011

The Preview Curvature Controller for a passenger car steering robot

Development of a closed-loop path controller for repeatable vehicle dynamics testing

Master's Thesis in the Master's programme Automotive Engineering and Systems, Control and Mechatronics
KLAS OLSSON, CARL SANDBERG

Master's Thesis 2011:41
ISSN 1652-8557
Department of Applied Mechanics
Division of Vehicle Engineering *and Autonomous Systems*
Chalmers University of Technology
SE-412 96 Göteborg
Sweden
Telephone: + 46 (0)31-772 1000

Cover:
Figure showing the steering robot and car performing a double lane change manoeuvre.

Department of Applied Mechanics
Göteborg, Sweden 2011

The Preview Curvature Controller for a Passenger Car Steering Robot
Development of a closed-loop path controller for repeatable vehicle dynamics testing
Master's Thesis in the Master's programme Automotive Engineering
KLAS OLSSON, CARL SANDBERG
Department of Applied Mechanics
Division of Vehicle Engineering and Autonomous Systems
Chalmers University of Technology

ABSTRACT

Purpose – Saab Automobile AB is planning to extend the use of steering robots to increase the repeatability and effectiveness of vehicle dynamics testing. A robot from Vehico GmbH has been considered for this task and to extend the use of the robot, from today's open loop control, a closed loop path controller has been developed in this master thesis. The new controller uses GPS and inertia sensors to guide the vehicle along a predefined path. The controller can also perform superimposed closed loop control of open loop manoeuvres to enhance safety during testing.

Procedure – After an initial literature review the controller was developed as a Simulink model. IPG CarMaker was used to simulate the vehicle dynamics and evaluate the performance of the controller. When the controller had been developed in Simulink it was converted to C-code and implemented into the robot software. Physical vehicle testing was performed to further evaluate performance and correlate simulations and reality.

Results – The developed controller projects a preview point onto the track ahead of the vehicle. The required path curvature to reach the preview point is calculated and used as input to the controller. A predefined map of steering angle versus curvature and vehicle speed is used to calculate the required steering angle. Calibration of the controller is done by performing a simple steady state circle manoeuvre. The path following performance is very good all the way up to the limit of adhesion. The actuation is smooth and the path error rarely exceeds 1 m even at lateral acceleration levels of 10 m/s^2. Most importantly good repeatability between the runs is achieved.

Key words: Path control, steering robot, closed loop control, vehicle dynamics, lateral control.

Utveckling av ett styrsystem med återkoppling för en styrrobot i passagerarfordon.
Examensarbete inom Masterprogrammen Automotive Engineering och Systems, Control and Mechatronics

KLAS OLSSON, CARL SANDBERG
Institutionen för tillämpad mekanik
Avdelningen för Fordonsteknik och Autonoma System
Chalmers Tekniska Högskola

SAMMANFATTNING

Syfte – Saab Automobile AB planerar att utöka användningen av styrrobotar vid fordonsdynamiska tester för att öka effektiviteten och repeterbarheten. Till detta är en styrrobot from Vehico GmbH tänkt att användas. För att utöka funktionaliteten hos denna robot har i detta arbete en closed-loop controller för banföljning utvecklats. Den nya regulatorn använder GPS, gyron och accelerometrar för att leda fordonet längs en fördefinierad bana. Regulatorn kan också övervaka open-loop tester för att öka säkerheten vid dessa.

Metod – Efter en inledande litteraturstudie utvecklades en regleralgoritm i S*imulink*. IPG CarMaker användes för att simulera fordonets dynamik och därmed utvärdera regulatorns prestanda. Den utvecklade regulatorn har skrivits om till C-kod och implementerats i styrrobotens realtidsdator. Fysiska tester har också gjorts för att utvärdera prestandan hos regulatorn och för att bekräfta att simuleringsresultaten stämmer.

Resultat – Den utvecklade regulatorn projicerar en punkt på banan framför bilen. Den kurvatur som bilen ska ha för att träffa denna punkt på banan räknas ut och ges som insignal till regulatorn. En fördefinierad funktion som översätter önskad lateral acceleration till rattvinkel används för att räkna ut styrsignalen. Denna funktion tas fram genom att köra i en cirkel med långsamt ökande hastighet. Prestandan hos regulatorn är mycket bra, även då däcken är mättade. Kontrollsignalen är inte ryckig och det absoluta felet överstiger sällan en meter, även vid 10 m/s^2 i lateral acceleration. Viktigast är att repeterbarheten är mycket god.

Nyckelord: Banföljning, styrrobot, closed loop styrning, fordonsdynamik, lateral kontroll

Contents

Preface

A closed loop path controller for an automotive steering robot called *The Preview Curvature Controller* has been developed. The path controller extends the range of use for the robot to increase the quality and effectiveness of vehicle dynamics testing.

The work has been carried out from January to June 2011 at *Saab Automobile AB* by the students Klas Olsson and Carl Sandberg from *Chalmers University of Technology*. An equally important partner in the project has been Vehico GmbH who has provided the steering robot for which the controller is developed, as well as supporting the development of the controller. The thesis is a master thesis within the masters programmes *Automotive Engineering* and *Systems, Control and Mechatronics.* The thesis is done at the department of *Applied Mechanics*.

We would like to thank the following persons for their invaluable support:

Our supervisor, ***Matthijs Klomp*** for his dedication and support of the project

Our examiner, ***Mathias Lidberg*** for concern of our work load

Jörg and ***Lothar*** from ***Vehico***, for trusting us with their robot

Saab Mätservice, for support with measurement equipment

Jörg Lemnitzer, for help with testing

Gabriel Palmenäs, for help with measurements

Modelon AB and ***IPG Automotive GmbH***, for providing CarMaker licenses

Göteborg July 2011

Klas Olsson

Carl Sandberg

Notations and Definitions

Roman upper case letters

A	State Matrix
B	Input Matrix
C	Output Matrix
E_i	Input error to controller
V	Vehicle velocity
K	Kalman factor
K_i	Controller gain
L_x	Length in meters, indexed
R_x	Radius, indexed
X	Position in x, global
Y	Position in y, global

Roman lower case letters

y_{lim}	Track lateral boundary during open loop manoeuvre
x_i	Actual state in state space representation, indexed
$\hat{x}_i$	(Kalman) Estimated states in state space, indexed
y	Output from state space representation
t_{step}	Compensation time for lateral acceleration response

Greek lower case letters

δ_{hw}	Hand wheel angle
ψ	Car yaw angle
φ	Track angle
ξ	Angle of curved track segment

Vectors

$\vec{e}$	Vector from track to preview point, normal to track
$\vec{w}_p$	Vector from start of straight or centre of curve to preview point
$\vec{w}_t$	Vector from start to end of straight segment
$\vec{w}_0$	Vector from curve centre to start of curve segment
$\vec{w}_1$	Vector from curve centre to end of curve segment

Definitions

Track	The track that the car is supposed to follow

Path The path that the car actually travels. The difference between the track and the path at a given instance is the position error.

Subscript Letters

c	Vehicle
p	Preview point
t	Nearest point on the track from the preview point
0	Circle centre of feedforward curvature
s	Track segment
sb	Track segment beginning
se	Track segment end
r	Circle centre of track arc
ss	Steady state
cc	Curvature control

1 Introduction

To complement human test drivers Saab Automobile is planning to use a robot to control steering during vehicle dynamics testing. Using a robot improves repeatability and the possibility to perform very precise manoeuvres, such as the sine with dwell manoeuvre (see chapter 2.4.3). It is also beneficial to use a robot in testing that is dangerous or very uncomfortable. A robot is also capable of performing inputs faster than a human driver. This enables evaluation of not yet existing (in the test vehicle) active safety systems such as active steering.

The intended robot is delivered by Vehico GmbH Vehico (2011) and is currently only capable of open loop control of the steering i.e. following a pre-set steering profile. To extend the functionality of the steering robot a controller that uses the position of the car from a GPS system (chapter 2.2.1) as input to guide the car along a path has been developed. Compared to GPS navigation systems available in vehicles today the developed controller turns the wheel instead of telling the driver to turn. Within this thesis the controller will be referred to as a closed loop path controller. Longitudinal control of the vehicle, i.e. accelerating and braking, is not handled by the developed closed loop controller.

Similar controllers are often referred to as driver models when used in vehicle dynamic simulations. However, an important distinction from a classic driver model is that the closed loop path controller aim at performing optimal vehicle control, with little consideration to human resemblance.

1.1 Procedure

The thesis involves development and evaluation of a feedback steering controller both in simulation and in-vehicle testing. The following steps will be performed during the development:

1. Literature study. Earlier research on autonomous vehicle control is studied to give inspiration about how to develop the closed loop path controller.
2. Development of the controller in Matlab/Simulink. Vehicle simulation is done in CarMaker (chapter 2.6) from IPG Automotive. By connecting Simulink to CarMaker the performance of the controller is evaluated.
3. The developed controller is converted to C-code which can run on the real-time computer controlling the steering actuator of the robot.
4. Performance of the controller is evaluated by in-vehicle testing. The results from vehicle testing are compared to simulation results.

1.2 Aim

This thesis aims to deliver a closed loop path controller for steering that uses GPS (chapter 2.2.1) and inertial measurements (chapter 2.2.2) as input signals. The controller should be implemented to control the Vehico steering robot (chapter 2.1) and tested in a test vehicle. The following tasks should be possible to perform with the steering robot and the closed loop controller:

- Follow a path at a wide range of speeds. This includes driving at the limit of adhesion and repeatability is more important than absolute path following precision.

- Monitor an open loop manoeuvre such as the sine with dwell, and abort the test and steer the car back if the car is about to run off the track.
- Compensate for lateral drift of the vehicle in a sine sweep manoeuvre (chapter 2.4.2) without affecting the frequency content of the steering control signal.
- Combine and switch between open and closed loop control within a test manoeuvre.

The requirements on the controller performance have been set to fulfil the needs of future users. In order to be integrated into the current user interface and combined with open loop manoeuvres certain requirements are also set on the controller structure. These requirements, applicable primarily to path following, are summarized below:

- A segment shall be simple to define. The target track will be made up of several segments.
- The controller shall handle each segment of the track individually. This means for example that no account will be taken for an upcoming tight corner while on a straight.
- The controller shall be able to cope with a non-constant speed, as the speed is to be controlled by a human driver.
- The controller shall be able to handle sudden disturbances, both to the input signals and to the vehicle itself.

1.3 Delimitations

The following restrictions are made to limit the scope of the thesis:

- Longitudinal control is performed by a human driver.
- No new user interface is developed, the interface provided for open loop control of the Vehico robot is used.
- The path is predefined by the user, i.e. no path planning is performed online.
- Already existing vehicle models in CarMaker will be used for evaluation of the controller during the development phase.

2 Background

This chapter will present the properties of the three main systems involved in the thesis, namely the steering robot, a passenger car and the measurement system. The manoeuvres, also mentioned in section 1.2, that the robot should perform are explained in greater detail in chapter 2.4. Manoeuvres important for system identification are also explained. Finally, theory for non-linear control is presented since this is important in order to achieve precise lateral vehicle control up to the limit of adhesion.

2.1 The steering robot

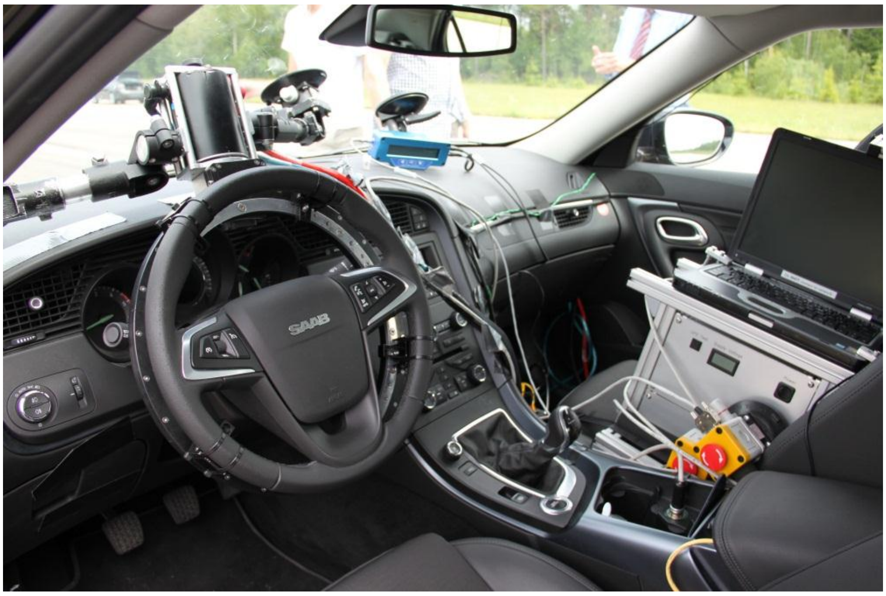

Figure 1: The vehico steering robot when installed in a SAAB 9-5. The electric drive mounted to the windscreen with vacuum cups is connected to the original steering wheel via a geared ring. The grey box on the passengers seat is the real time computer and on top of it the windows computer used to define meanouvres.

The steering robot actuating the developed closed loop controller is a S1200 steering robot from Vehico GmbH. The robot consists of an electric drive unit that is mounted at the windscreen of the vehicle using vacuum cups. The drive is connected to the original steering wheel via a geared ring mounted behind the original steering wheel. The steering wheel can be operated as usual when the robot is not active and therefore the vehicle can be controlled by a driver until the start of a robot controlled manoeuvre. The robot is controlled by a real time computer running a Linux based real time operating system, RTAI. The real time computer generates a control signal which is transferred into a pulse-width modulated signal by power electronics fed with power from the 12 volt system of the vehicle it is installed in.

The robot is programmed by the test engineer using a windows based graphical user interface running on an external computer. This computer communicates with the real time computer over an Ethernet connection. The manoeuvre to be performed is defined using a simple scripting language in which a command is given in the following form:

```
manoeuvreName(parameter1,..., parameterN)
```

Several commands can be combined to build an arbitrary manoeuvre. The real time computer of the steering robot has a CAN interface which can be used for connection of external sensors.

Vehico (2011)

2.2 Signals and sensors

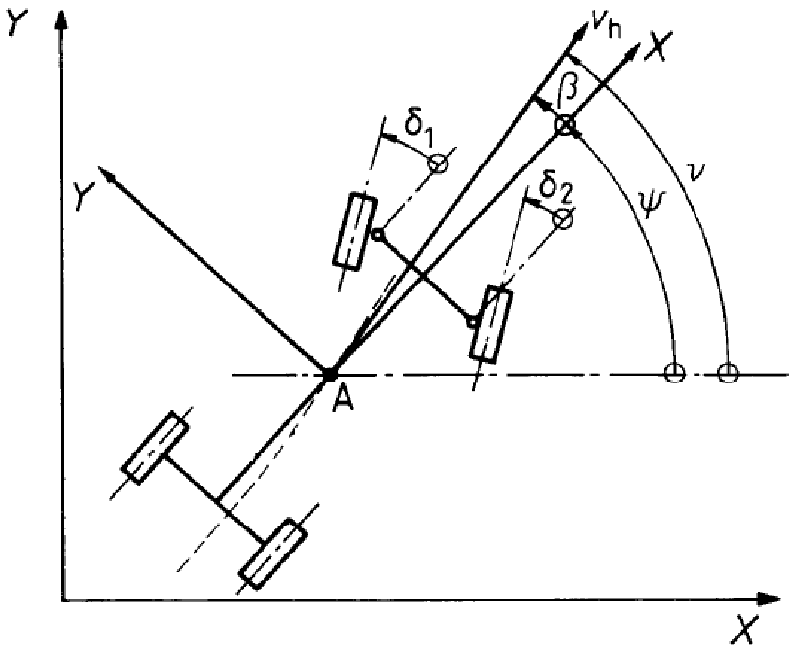

Figure 2: Definition of signals used as input to the controller. The main inputs to the controller are the position of the vehicle and its heading angle ψ. The speed in the course direction v_h is also used by the controller.

The two main inputs to the controller, the position and heading angle of the vehicle are measured by a GPS system and an inertial measurement unit (IMU) respectively. The speed of the vehicle in its course direction (v_h, Figure 2) is also measured by the GPS. To improve the position measurement from the GPS, measurements from the IMU has been taken into account using the method described in chapter 2.2.3.

2.2.1 Global positioning system, GPS

The GPS system relies on satellites with very exact on-board clocks to determine the position of a receiver. By comparing the time it takes for transmissions from different satellites to reach the receiver a position is calculated by triangulation, as the satellites’ positions are known. Because the signal travels at the speed of light the difference in time between when the signals reaches the receiver is very small, and hence the system is very sensitive to disturbances, resulting in an accuracy of about 3 meters. This accuracy can however be greatly increased by using Real Time Kinematic (RTK) correction. In RTK a secondary GPS receiver is placed in a base station with a known position. This base station transmits a correction signal, calculated from the error between actual position and GPS position, to the GPS receiver in the moving object. Using RTK an accuracy of about 2 centimetres is achieved.

Wikipedia-GPS (2011)

The GPS system used within this thesis is a VBOX III system from Race Logic. It has an update frequency of 100 Hz and provides the location of the receiver as well as an exact velocity measurement. The VBOX III also supports use of GPS base stations to improve the accuracy down to 2 cm though this has not been available during this thesis.

Race_Logic (2011)Race_Logic (2011)

2.2.2 Inertial measurement systems

An inertial measurement unit (IMU) measures its orientation angles and acceleration with gyros and accelerometers. These measurements can be used to calculate the position of the sensor by integration. A standalone inertial navigation system is, because of the integration, very sensitive to gyro drift and acceleration measurement inaccuracy, leading to an error that grows over time. This method of determining position is however a good complement to GPS position measurements since it can provide a position measurement without relying on satellite connections. The IMU is also necessary to provide the heading angle of the vehicle, since the GPS system can only provide the course angle.

Wikipedia-IMU (2011)

The IMU used within this thesis is an iDis-FMS inertial measurement unit with fibre optical gyros. The system has a very low angular drift of one degree per hour and uses GPS heading to calibrate the yaw angle. Optionally it can be equipped with GPS-RTK (see chapter 2.2.1) functionality and connected to a base station, but the unit used within this thesis does not have this option.

iMAR_GmbH (2006)

2.2.3 Kalman filtering and Sensor fusion

To make the best use of the available measurement data from the GPS system and the IMU a kinematic filter based on Kalman filtering theory can be used to fusion the sensor data. This is important since the raw GPS position signal is sensitive to disturbances from the surroundings that can lead to a step in the position signal. With this fusion of the signals the position signal from the GPS and the predicted position at the next time instance calculated from the north-south and east-west accelerations (measured by the IMU) are combined.

This method is applied to the position measurement only; the heading angle measurement from the inertial measurement unit is used as it is, as well as the speed measurements from the GPS.

A Kalman filter is a state observer for the states x,

$$\dot{\hat{x}} = A\hat{x} + Bu + K(y - C\hat{x}) \tag{1}$$

A is here the system matrix, where the factor K determines how the measured input y is weighted versus the previous estimate $C\hat{x}$. The weight factor K, called the Kalman factor, is calculated, based on process and measurement noise (R_1 and R_2) assumptions so that the estimation error is minimized, as:

$$K = PC^T R_2^{-1} \tag{2}$$

where the matrix P is the solution to the steady state Riccati equation:

$$\dot{P} = AP + PA^T - PC^T R_2^{-1} CP + R_1 \tag{3}$$

Relative to the assumptions on noise (R_1 and R_2) the Kalman filter will be the optimal observer.

In the kinematic filter used in this thesis the following state space model is used for motion in one dimension:

$$\left.\begin{aligned} \dot{x_1} &= x_2 \\ \dot{x_2} &= x_3 + a \\ \dot{x_3} &= v \end{aligned}\right\} \quad y = x_1 + w \tag{4}$$

where x_1 is the position, x_2 the velocity and x_3 the acceleration. The measured acceleration a is affected by white noise v and the GPS measurement, y, by a wideband noise w.

By using the state space equations in Equation 4 and estimations of noise, a Kalman factor (Equation 2) can be calculated. The observer state space model (Equation 1) can then be computed and discretized to run at a set frequency. The output from this observer is a position measurement in one dimension, hence two equivalent filters has to be run in parallel, one with position and acceleration in the global X direction and one with measurements in the global Y direction (see Figure 2).

When the filters are initialized the current position and speed, measured by the GPS, are used to set the initial conditions of the states x_1 and x_2. Speed measurement is only used for initialization, not as input to the filters while running.

Schmidtbauer (2010), Karl J. Åström (1997)

2.3 Lateral dynamics of the vehicle

The lateral dynamics of a vehicle can be divided into three main modes of operation. The first mode, steering at low levels of lateral acceleration, can be considered a stable linear system. A linear bicycle model can be used to calculate the required steering angle as a function of cornering radius at constant vehicle speed, Figure 3, equation 5. The understeer gradient K_{us} is considered a constant depending upon weight distribution and cornering stiffness, assuming linear tyres and no load transfer.

$$\delta = \frac{L}{R} + K_{us}\frac{V_x^2}{gR} \tag{5}$$

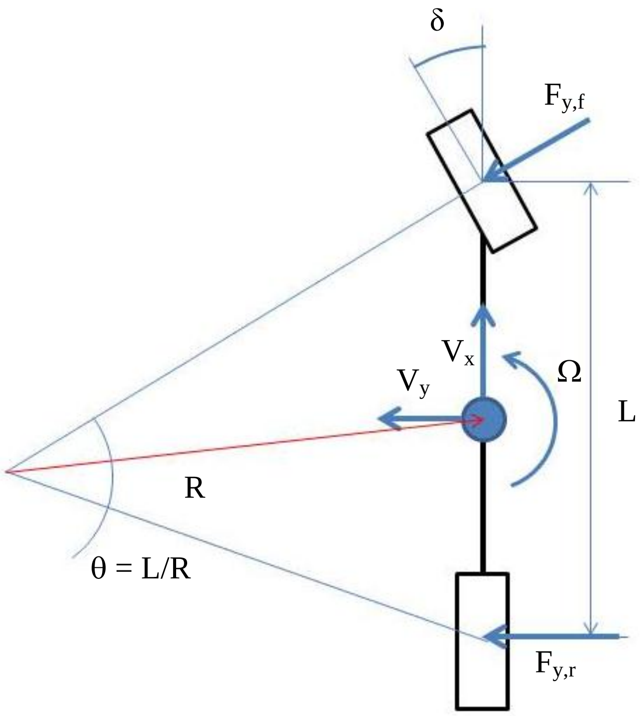

Figure 3. The bicycle model. Used as a vehicle model with no respect to lateral load transfer.

At higher lateral accelerations, demanding more side force from the tires, the system becomes highly nonlinear. The main cause of this non-linearity is the limited available tire side force. One common way to model the tyre side force versus slip angle is to use the Magic Tyre Formula Pacejka (2005), Equation 6. A typical plot of side force versus slip angle is shown in Figure 4. As seen the curve is highly nonlinear for high slip angles and even decreasing for very high slip angles. Equation 6 is valid only for zero load transfer and no longitudinal forces. One way of modelling combined slip with load transfer is shown in Equation 7. The D parameter sets the maximum lateral force, primarily depending on vertical and lateral force for a specific tyre. The B, C and E parameters sets the cornering stiffness and nonlinear behaviour.

$$F_{y0} = \sin\left[C\,\mathrm{atan}\big(B\alpha - E(B\alpha - \mathrm{atan}(B\alpha))\big)\,\right] \tag{6}$$

$$F_y = F_{y0}D \tag{7}$$

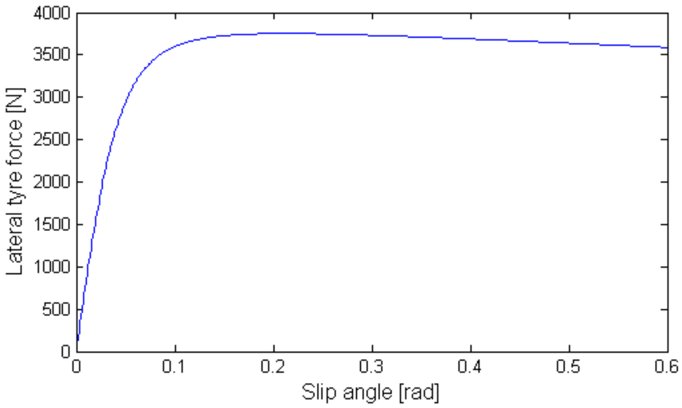

Figure 4. Tyre lateral force versus slip angle according to the Magic Tyre Formula.

The third mode is transient cornering when the system is non-linear and time dependent. Effects such as tyre relaxation, acceleration forces, damping and the response time difference between front and rear axle make large differences to the dynamic behaviour of the vehicle.

The lateral dynamics of a variety of cars and setups will be investigated in two ways; step steer response and steady state circle driving. These two manoeuvres will give insight to how the vehicle responds and how this might be compensated for in the controller. The step response and circular driving is done with IPG CarMaker using IPG-Driver for control. To follow a track lateral acceleration is more important than the yaw motion since it describes the translation of the vehicle, given relatively low side slip. The simulation results are therefore presented as lateral acceleration versus steering angle.

Of course there are an abundance of manoeuvres that could be performed to get deeper knowledge of the lateral dynamics. However, since the aim is to avoid the need of advanced mathematical vehicle models the gain in investigating more manoeuvres are considered small.

2.3.1 Step Response

To learn how different vehicles react to a step steer and how the response time varies with longitudinal speed and steering amplitude three different vehicles were tested in simulation; a small front wheel driven car (Ford Focus) with two sets of tires and a large front wheel drive car (Saab 9-5). Table 1 shows how the response time varies with the steady state lateral acceleration. The response time is defined according to ISO-7401 as the time from when 50% of the steering angle is reached until 90% of the steady state lateral acceleration is reached. The standard suggests a steer input of maximum possible velocity, preferably by a steering robot. The maximum speed of the Vehico robot is roughly 21 rad/s though for calibration a speed of 10 rad/s has been used. The throttle is held constant once the desired speed is reached and the steering input is applied. The entry speed is 90 km/h and the steering angle after the step is the steering angle which gives the corresponding steady state lateral acceleration.

As can be seen the choice of tires has the most significant effect on the response time. If one considers the average response time of 0.41 seconds from these test, that would correspond to an overshoot of 10 meters until 90% of the lateral acceleration is reached. This test shows that in order to achieve high performance it is necessary to compensate for the response time of the car in the controller. How this is done is explained in chapter 4.5.

Table 1. Response time (ISO-7401) for constant vehicle entry speed and varying steady state a_y.

V = 90 km/h	**$a_{y,ss}$ = 4 m/s^2**	**$a_{y,ss}$ = 6 m/s^2**	**$a_{y,ss}$ = 8 m/s^2**
Ford Focus, R17	0.34 s	0.40 s	0.39 s
Ford Focus, R15	0.50 s	0.50 s	0.44 s
Saab 9-5, R17	0.36 s	0.42 s	0.30 s

2.3.2 Nonlinearity in Steady State

The steady state behaviour was tested for two different cars (Saab 9-5 and BMW 5-series) on two different sized circles (R40 and R80) at two different friction levels (μ=1 and 0.6), in total eight test setups. The results for the Saab can be seen in Figure 5. The cars are driven with a constant longitudinal acceleration of 0.1 m/s^2 until the set radius cannot be held. Figure 5 shows the result from simulating the front wheel driven Saab 9-5. For the high friction case a linear controller based on Equation 24 would be sufficient up to around 7 m/s^2 and up to 4.5 m/s^2 for low friction. For driving in the linear region recalibration would not be necessary for changing friction. For driving on the limit in the non-linear region calibration would however be necessary. The rear wheel drive BMW has a more linear behaviour over the available range of lateral acceleration.

The experiment shows that a linear controller together with feedback probably would be sufficient to give accurate control up to around 80% of the maximum lateral acceleration. Depending on the vehicle and surrounding circumstances a non-linear controller would probably be necessary for more precise steering at the limits of handling.

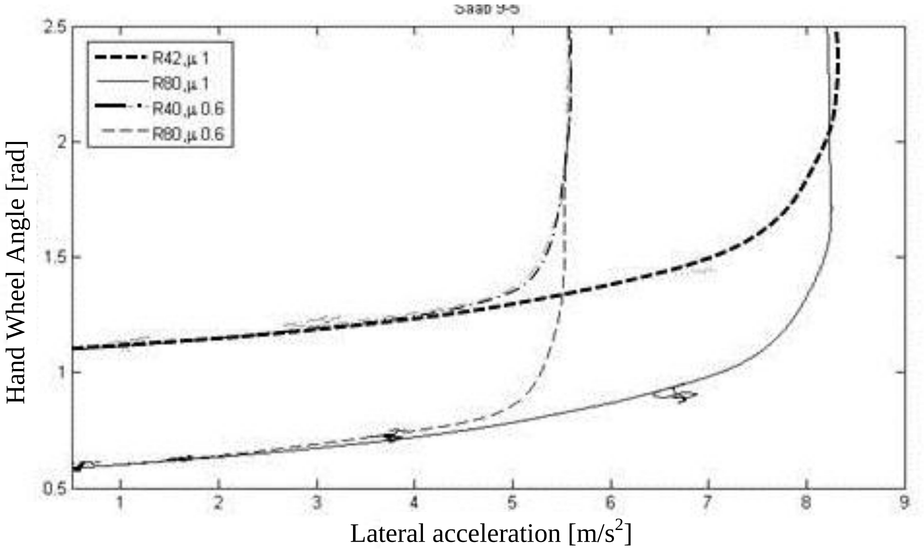

Figure 5. Steady state circle driving with Saab 9-5 on different radius circles with different friction. The required steering angle is translated vertically with a change in radius and horizontally with a change in friction.

2.4 Manoeuvres to be performed

This section presents the manoeuvres that the new steering robot controller will be developed and evaluated for. These involve both closed loop control and open loop with superimposed closed loop control.

2.4.1 Path following

Path following is the most advanced manoeuvre the robot can perform. It can consist of any arbitrary, although predefined, track that the car can physically be driven on.

To follow the track also at the limits of adhesion demands a controller that can adapt to the non-linearity of the vehicle. Even if no path planning is performed online in the controller it is crucial that the controller has a good strategy of how to maintain the car on the track in a smooth yet precise way. To calculate a reference steering angle there are two main tasks that the controller needs to perform continuously:

1. Calculate the distance and heading to the track, which becomes the controller input error. One major issue with calculating the error is to decide on exactly which point on the track the position should be compared against.
2. In the controller create a reference steering output value that makes the car return to the track in a stable, smooth and fast manner.

2.4.2 Sine Sweep

During a sine sweep the steering wheel is moved in a sinusoidal movement with increasing frequency. This is normally an open loop manoeuvre which requires a wide track to ensure that the vehicle does not leave the track. With an overlaid closed loop control the aim is to keep the vehicle in proximity to the centre of the track while affecting the open loop behaviour as little as possible. The sinus sweep is done to evaluate the frequency response of the vehicle. From measuring steering angle, lateral acceleration and yaw rate the transfer functions from steering input to lateral acceleration and yaw rate respectively can be estimated. The transfer functions are commonly presented in bode-plots showing gain and phase for a given interval, typically 0.5 to 4 Hz. Frequency analysis will be done to ensure that the feedback control does not affect the results.

2.4.3 Sine with dwell

The US *Federal Motor Vehicle Safety Standard* (FMVSS) act number 126 requires all vehicles with a weight below 4536 kg sold in the United States after 2010 to be equipped with an Electronic Stability Control (ESC) system. The ESC performance must fulfil certain requirements which are assessed by the so called sine with dwell manoeuvre.

The manoeuvre consists of steering input defined by a sine wave with the frequency 0.7 Hz and a dwell time of 0.5 s in the second steering direction see Figure 6. The speed when starting the manoeuvre is 80 km/h. A series of the sine with dwell manoeuvre are conducted with the amplitude of the sine wave starting at a steering wheel angle of $1.5\delta_A$, where δ_A gives a lateral acceleration of 0.3g in steady state. The amplitude is increased by 0.5 δ_A each run until a steering angle above 270 degrees is reached. The vehicle tested must at all amplitudes within the test series fulfil a set of criteria related to responsiveness and end of manoeuvre stability.

The steering wheel angle in this manoeuvre must be controlled by a steering robot for accuracy and repeatability.

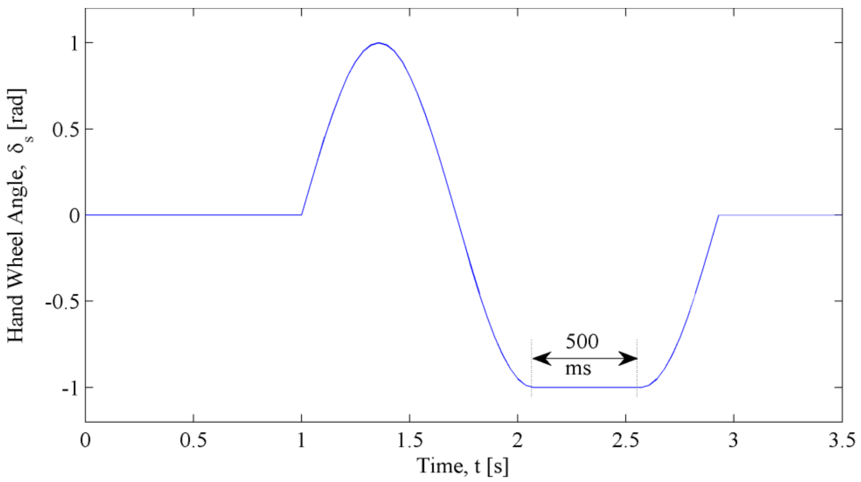

Figure 6. Sine with dwell steering input.

2.4.4 Steady State Circular Driving

Steady state circular driving is a good tool to evaluate the steady state handling characteristics of a vehicle. The ISO-4138 standard suggests three variants where steering angle, speed or cornering radius is gradually changed. The most common method, and the one considered in the thesis, is driving on a constant radius circle with slowly increasing speed. To be able to assume steady state the increase in lateral acceleration should not exceed 0.1 m/s^2/s. Because the driving is steady state it is relatively easy to identify how changes to the vehicle affect the dynamics. For most production vehicles it is a requirement that they maintain a stable behaviour in steady state conditions so that it is easy to control also for a less experienced driver. The steady state circle manoeuvre is also good for calibrating more advanced controllers; this is described in chapter 4.5.

2.5 Design methods for non-linear vehicle control

As a vehicle is well within its linear operating region at low speed cornering a controller could be designed with linear design methods at low speeds. However, at higher speeds the system becomes nonlinear. This makes it necessary to use nonlinear design methods. In the sections below three concepts for nonlinear control is presented. Since it is unwanted to have to rely on advanced mathematical vehicle models for the control any method involving this is not considered.

2.5.1 Gain scheduling

The first concept for the controller was to use a gain scheduling as the design method. This method involves linearizing the system in a number of operating points and then applying linear design methods to the controller in each operating region. This is a feasible approach and the resulting controller would respond quickly to a change in operating point. The problem with this design method is that a new controller would have to be designed for each new vehicle since its dynamics is different. To use the robot with this kind of controller in a new vehicle would then require the operator to tune the controller. This would of course take a great amount of time and require a more skilled operator.

2.5.2 Multiple Preview Proportional Control

This is a method described by Sharp, Casanova and Symonds (2000) for controlling a race car replicating an optimal lap at a race track. The path error is estimated through several preview points ahead of the car, Figure 10. Each error has an individual gain and saturation limits, see controller layout in Figure 7. Although the individual gains of the controller are constant the controller will be nonlinear because of the saturation limits of the different gains. These limits the steering to not exceed the saturation limits of the tires when driving at high levels of lateral acceleration. The state feedback seen in the bottom of Figure 7 is primarily for yaw stability.

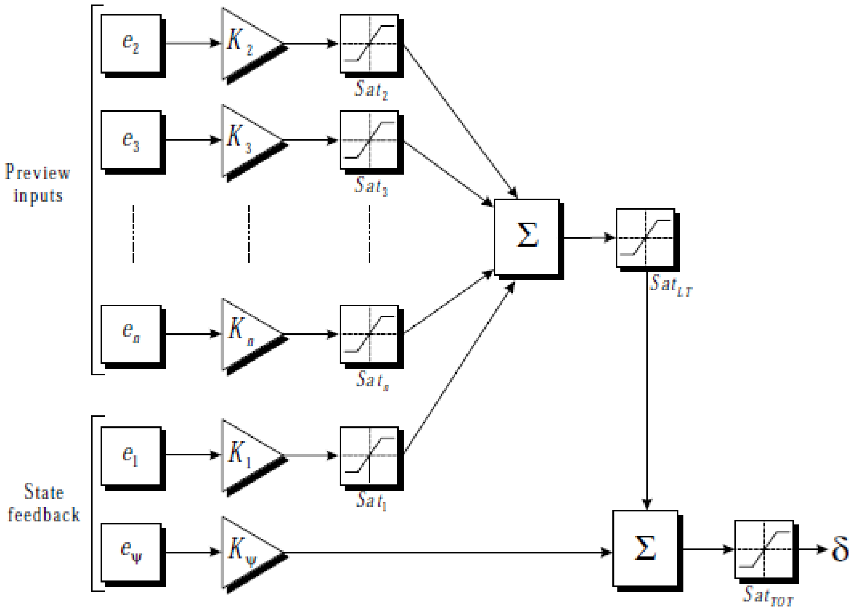

Figure 7. Steering angle control scheme with saturation functions, from Sharp, Casanova and Symonds (2000). Previews errors from multiple points ahead of the car is used to generate a steering angle control signal.

2.5.3 Anti-windup design

As an integrating controller will make a sum of the error over time this sum will grow as long as the reference signal is not tracked. When saturating an actuator, in this thesis the tires, an increase in control signal will not have any effect on the system. The integrator error will however continue to build up, making it very large if the actuator is saturated for a long time. When the systems starts to move towards the reference value the integrator error will continue to increase until the current error is zero. The control signal will therefore be large a long time after the actuator saturation leading to a poor tracking performance. This phenomena is called integrator windup. The simplest way of dealing with this problem is to stop integrating the error when the actuator is saturated. This is one example of anti-windup design.

Karl J. Åström (1997)

2.6 IPG CarMaker

In the thesis all vehicle simulations have been done with the commercial software *CarMaker* from *IPG automotive*. The simulation software includes detailed nonlinear vehicle dynamic models and also an advanced driver model, *IPGDriver*. The main use of *CarMaker* with *IPGDriver* is to perform what *IPG* calls *Virtual Testdriving*, decreasing the need for expensive physical test driving.

CarMaker can be integrated with *Simulink* to enable software in the loop testing of advanced functionality, such as new electronic stability programs (ESP) or other active safety functions. The Simulink interface has in this thesis been used to transfer the control of the steering wheel angle from *IPGDriver* to an external controller. In Simulink all data from the simulation, such as wheel speeds, lateral acceleration and the vehicle position, is available to use as an input to the Simulink function.

IPG_Automotive_GmbH (2010)

3 Literature Review

The literature review has involved research within two main areas; how to define position relative to the track and how to design the control logics, from position error to steering wheel angle. Primarily, literature about design of controllers capable of performing track following at high levels of lateral acceleration has been considered. It has also been important to evaluate how easily the controller can be adjusted to suit different cars without spending too much time on tuning and calibration.

3.1 Track Models and Path Planning

As Plöchl and Edelmann (2007) points out in their extensive technology review on driver models there are two main types of track following driver models; those that follow a pre-defined race line and those that involve path planning knowing the track boundaries.

Kelly and Sharp (2010) defines the track as gates which the vehicle must pass through, see Figure 8. This way of describing the track is a good way of describing performance driving at a track or a manoeuvre such as a double lane change. Although the current thesis does not involve path planning this method of defining the track can be interesting for further development of the robot controller.

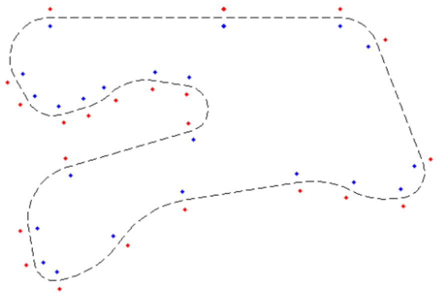

Figure 8. Track defined by gates.

Casanova (2001) defines the track as a function of the distance travelled since the start of a manoeuvre. In his PhD thesis a method of reconstructing a racing line from measured data is presented. Casanova uses the lateral acceleration of the car to determine the curvature of the race line, k_t, knowing that

$$k_t(t) = \frac{1}{r_t(t)} = \frac{a_y(t)}{V_x^2(t)} \tag{8}$$

where r_t is the track radius, a_{vy} is the lateral acceleration and V_{vx} is the longitudinal velocity. From this the track angle Ψ_t is calculated from

$$\psi_t(t) = \int_0^t k_t(t) \cdot V_x \cdot dt \tag{9}$$

The heading angle is then used to calculate the global position of the car at time *t* using the following two relationships':

$$x_t = \int_0^t \cos(\psi_t(t) \cdot V_x(t) \cdot dt \tag{10}$$

$$y_t = \int_0^t \sin(\psi_t(t) \cdot V_x(t) \cdot dt \tag{11}$$

For the robot controller it is more interesting to pre-define a track by defining the function $k_t(t)$. In this way the current position of the car can be compared to where the car should have been if it had followed the track exactly. As described here the travelled distance does not take lateral vehicle drift into account (which makes the car travel longer than the ideal track), though compensation can be made to account for it.

For creating a pre-defined track Edelmann, Plöchl, Reinalter and Tieber (2007) uses similar computations as Casanova though they build the track in segments of straights, constant radius curves or clothoids, rather than an arbitrary varying curvature. They calculate the distance to the track as the closest point of the track compared to a preview point, without considering travelled distance.

3.2 Path Error Calculation and Controller Design

How to calculate the car's deviation from the reference track is very much dependent on how the track is defined. The error is often expressed in lateral deviation from the track, direction to the track and sometimes also angular error between car heading and the track. Already in 1953 Kondo presented a driver model for calculating error to a straight line, Kondo (1953). Figure 9 illustrates Kondo's definition of the error which is very similar to what is used for controlling the Vehico robot described later. He uses a certain preview distance in the vehicle's yaw direction to find a corresponding point on the track to which the angle and lateral distance is calculated.

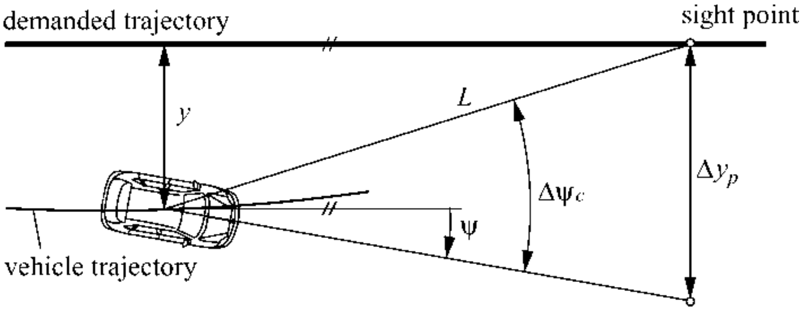

Figure 9. Kondo's shaft driver model. The distance between a preview point in the vehicle heading direction and the demanded track is defined as the path error.

One example of how to use the errors calculated in Kondo's model was presented by Reid (1983). Reid also includes curved track segments and calculates the steering angle to follow the current curvature of the track as well as compensating for the lateral and angular error, equation 12. K_x are the gains while ρ^* is the track curvature, $\psi_c$and y_p are as defined by Kondo in Figure 9.

$$\delta_c = K_c\rho^* + K_\psi\psi_c + K_y y_p \tag{12}$$

When considering driver models the Reid type of controller is often called a layered model because it includes an open loop feedforward control for path curvature and a second layer for feedback control of lateral error and heading. Donges (1978) presents a two layer model where desired and actual path curvature is added to the feedback layer. For managing critical situations Plöchl and Lugner (1999) adds a third layer to the controller. By observing sudden local deviations in i.e. yaw angle or yaw rate a stabilizing controller overriding the first two layers is used. This can for example help to avoid loss of control in an oversteer situation.

Tseng, Asgari, Hrovat, van der Jagt, Cherry and Neads (2005) has done physical experiments with an ABD steering robot (www.abd.uk.com) using a preview lateral error as control input. They experimented with using either heading angle or course angle for the preview. The course angle gave a more precise control while the heading angle gave a more stable response. The preview distance was based on time and their experiments found that good tracking was given by a short preview. A too short preview gave overshoot in the corners while a long one made the car cut corners too much.

The idea of comparing desired and actual path curvature can be used for adaptive control where the proportional gain is updated so that the controller learns the relation of steering wheel angle and path curvature. As the lateral acceleration is increased and the lateral dynamics becomes non-linear it is necessary to adapt the gain to the anticipated lateral acceleration. To rely only on feedback control may be too slow for such situations. One way is to use an advanced two track vehicle model to continuously calculate the required steering angle two follow a specified curvature at a certain speed. Falcone, Eric Tseng, Borrelli, Asgari and Hrovat (2008) uses this advanced type of vehicle model for model predictive control. By evaluating a sequence of future steering inputs the optimal sequence to follow the path can be found.

However, computations of nonlinear transient manoeuvres are difficult to achieve in real-time and also requires sophisticated vehicle/tire models for each car the controller is used for. An advanced mathematical model is also very sensitive to changes in the boundary conditions. Errors in estimating surface conditions and changes on the vehicle will compromise the performance of the model and the gains in using such an advanced model are lost.

Lin, Tang, Zhang and Yu (2005) points out that neural network types of control is popular for driver modelling both because of its tracking abilities and resemblance of a human driver’s way of thinking (Neural Networks are often used for artificial intelligence). However for this thesis human resemblance is not of interest and although the controller can have good performance it requires a lot of tuning. It is also very hard to predict the behaviour and analyse the stability because of the complexity and large number of tuning parameters.

To reduce the need of an advanced mathematical vehicle model and reduce the complexity compared to a neural network controller Xi and Qun (1994) suggest fuzzy logic control. The gain is changed based on number of rules observing the vehicle state and predicted path. By changing the rules and gain the controller can be tuned to different cars. The fuzzy logic controller has an advantage over the neural network because the rules are less interconnected and hence the output is easier to predict.

Sharp, Casanova and Symonds (2000) uses multiple preview errors as inputs to a proportional linear controller, described in chapter 2.5.2 and Figure 10. Each input of preview lateral error has a gain and saturation limits. The saturation limits makes the controller non-linear but the maximum influence from a single preview point is limited, increasing the performance. The multiple preview points ensures a smoother behaviour and that the track following is optimised over a finite distance rather than for a single preview point. The multiple preview controller demands extensive, vehicle specific, tuning to perform well.

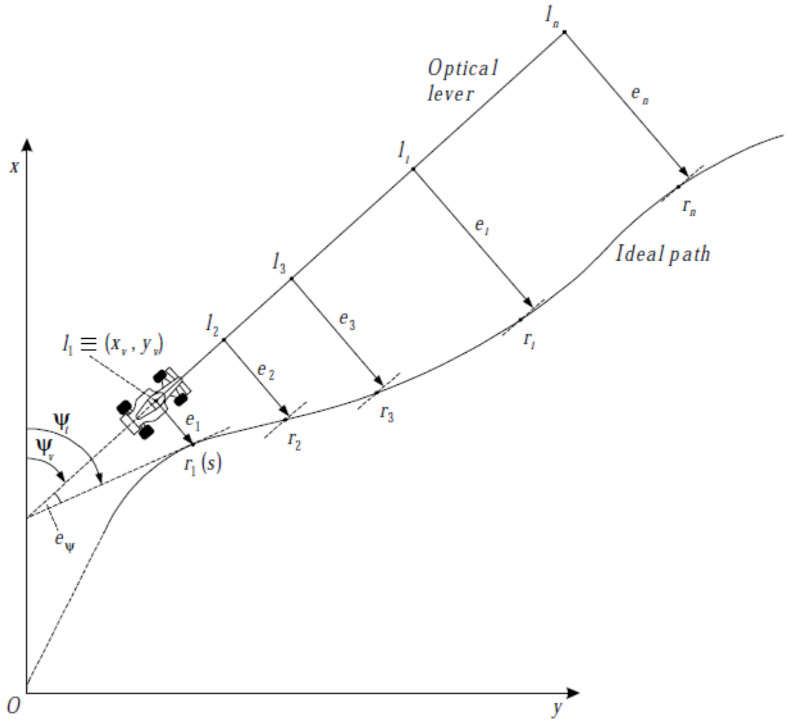

Figure 10. Multiple preview Sharp, Casanova and Symonds (2000). The error at several points ahead of the vehicle is used as the inputs to the controller (see Figure 7)

3.3 Summary of Literature Review

The literature review has shown that there has been plenty of research on driver models and there exists several ways to define the travel path and how to control the vehicle, especially considering high lateral accelerations. Studying these approaches gives a better understanding of what is important for controlling the Vehico robot and how the aim for this thesis is unique:

1. The track will be predefined, i.e. no path planning. Since the aim is to evaluate vehicle dynamics, creating an optimal race line is not of special interest.
2. The robot shall perform optimal lateral control of the vehicle; human resemblance is not of special interest.
3. Flexibility of the controller is a key issue. It needs to be very easy to adapt the controller to a large variety of passenger cars. This is a demand from Vehico in order to make the controller attractive to a wide range of customers.

Especially the demand for vehicle flexibility constrains which controller designs that are suitable for the Vehico robot. The neural networks, fuzzy logic and multiple preview are all controllers that have great tuning opportunities. However, this is also what makes them unsuitable since the tuning is time consuming and it is difficult to relate specific parameters to the steering behaviour. Controllers that rely on advanced mathematical vehicle models are also not wanted because it is difficult and time consuming to generate a good model for a new vehicle if there is none available.

4 The Preview Curvature Controller

Based on the literature review (chapter 3), initial testing in simulations and the demands set in chapter 1.2, the proposed controller, *The Preview Curvature Controller*, is a proportional controller using one preview point.

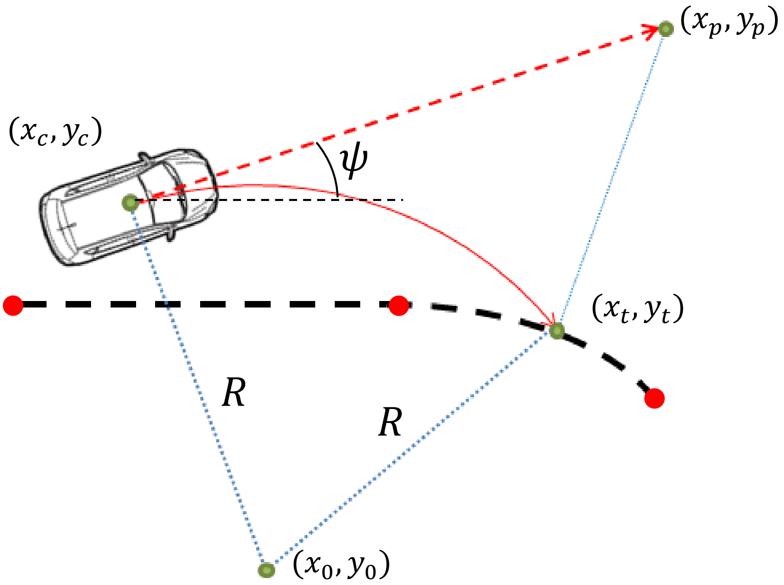

Figure 11. Definition of parameters used by *The Preview Curvature Controller*. The red points represents segment start/end points p_{sb}/p_{se}.

The controller (Figure 12) calculates the curvature needed to intersect the path at a preview distance ahead. This curvature is then the input to a feed forward controller that calculates the steering angle needed to follow the input curvature. The feed forward controller also uses the current speed of the vehicle to adapt the steering angle output to the expected lateral acceleration in the curve.

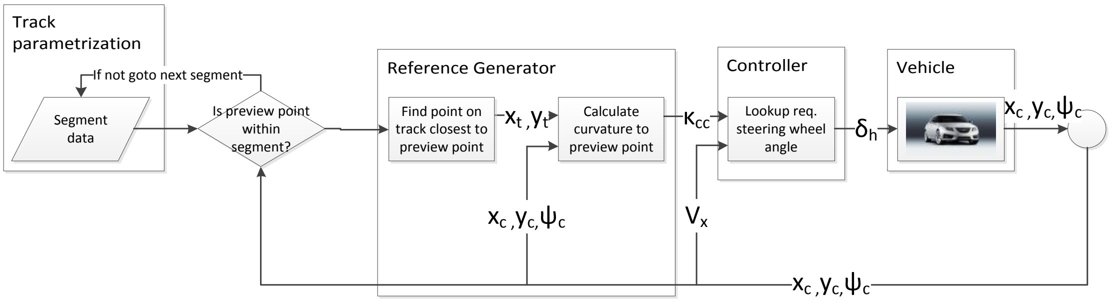

Figure 12: Structure of the *Preview Curvature Controller*.

In the following chapters the details of how the different parts of the controller works in detail will be presented.

4.1 Parameterization of the track

In order to calculate a reference signal to a path following controller the track to be followed must be parameterized in some way. The position and heading of the vehicle must also be related to the parameterized track in order to generate the control error. How these tasks are performed is presented here.

The track that the robot should follow is defined by a continuous set of straights and arcs, Figure 13. Each segment contains information of segment length, curvature and starting angle, Table 2. The position and starting angle of the first segment is specified by the user while the following segments starting point coincides with the end of the previous segment. In this way the user only has to define starting position of the track and length and curvature of each segment.

Table 2. Parameters used to define the two types of track segments, straights and curves.

Parameter / Segment	Length (L_s)	Radius (R_s) (positive)	Angle (ξ)
Straight	Meters	-	-
Curve	-	Meters	± Degrees

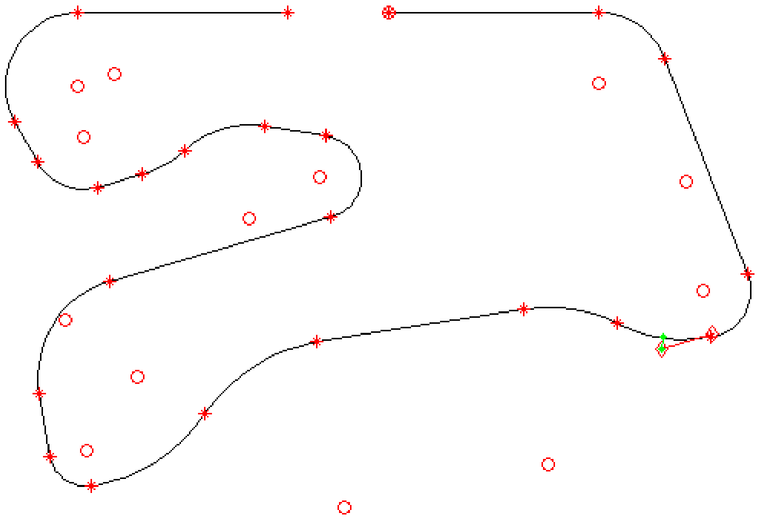

Figure 13. Track defined by continious straights and arcs. Arc centres represented by circles.

To give the required input to the controller and calculate starting position and angle of the next segment it is necessary to calculate the parameters presented in Table 3.

To calculate the end position, x_{se} and y_{se}, of a current straight segment, equation 13-14 are used. The point (x_{sb}, y_{sb}) is the beginning of the current segment, which has the length L_s and angle φ_s.

$$x_{se} = x_{sb} + L_s \cos \varphi_s \tag{13}$$

$$y_{se} = y_{sb} + L_s \sin \varphi_s \tag{14}$$

The end position of an arc in calculated by equation 15-16. The end angle is the starting angle φ_s plus the total curve angle ξ_s. R_s is the radius of the curve.

$$x_{se} = x_{sb} - \mathrm{sgn}(\xi_s) R_s [\sin \varphi_s - \sin(\varphi_s + \xi_s)] \tag{15}$$

$$y_{se} = y_{sb} + \mathrm{sgn}(\xi_s) R_s [\cos \varphi_s - \cos(\varphi_s + \xi_s)] \tag{16}$$

In order to decide if the preview point is within the current segment and to project the preview point onto the track it is necessary to calculate the arc centre for curved track segments, equation 17-18.

$$x_r = x_{sb} - R_s \sin \varphi_s \operatorname{sgn}(\xi_s) \tag{17}$$

$$y_r = y_{sb} + R_s \cos \varphi_s \operatorname{sgn}(\xi_s) \tag{18}$$

Table 3: Variables calculated in initialization state of each new segment.

Variable	Description	Comment
x_{sb}, y_{sb}	Start of segment	
x_{se}, y_{se}	End of segment	
$\vec{x}_s, \vec{y}_s$	Vector from start to end of segment	Only for straights
φ_{se}	Angle of track at end of segment	Only for curves
x_r, y_r	Centre point of curve	Only for curves

During the initial simulations simpler tracks where tried that were defined by only points, Figure 14 (Left), or straight vectors, Figure 14 (Right) , creating a sampled track. However, the simulations showed that it is very important to have a smooth and exact error signal which could not be realised by using these sampled tracks while maintaining real time simulation speed. The signal obtained with these tracks did give unstable controller behaviour.

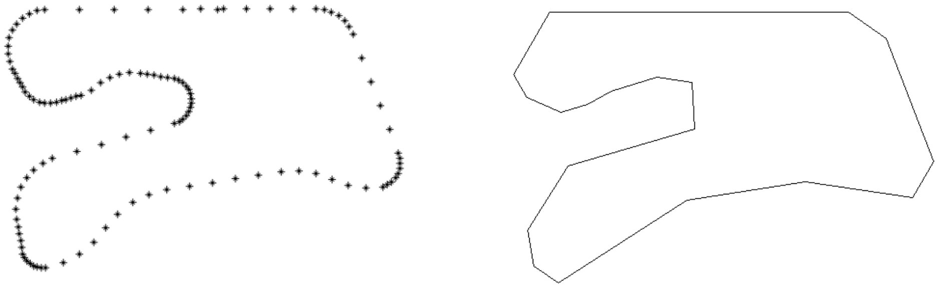

Figure 14. (Left) A track defined by points, many points are needed, especially in corners. (Right) A track defined by straight segments, here many short straights are needed to give a good representation of a curve.

The track definition used is continuous considering position and angle. To also have continuous radius it was considered to include clothoids, a curve of continuously increasing or decreasing radius. However, it was concluded that feedforward of the track curvature was unnecessary and since clothoids requires numeric integration an entirely continuous signal cannot be achieved.

4.2 Check if Preview Point is within Segment

Since the controller only considers the position of the preview point when calculating the steering angle this is the point that is compared to the track segments, rather than comparing the vehicle position to the track. The check of whether or not the preview point is within the current segment requires different strategies depending on if the current segment is a straight or a curve.

Line segment

The line segment s_i is described by the vector $\vec{w}_t$, from its start point to end point. By projecting $\vec{w}_p$, the vector between the starting point of the segment and the preview point, onto $\vec{w}_t$ and normalizing the ratio λ is calculated.

$$\lambda = \frac{\vec{w}_p \cdot \vec{w}_t}{|\vec{w}_t|^2} \tag{19}$$

$$\vec{w}_p = \begin{bmatrix} x_p - x_{sb} & y_p - y_{sb} \end{bmatrix}, \qquad \vec{w}_t = \begin{bmatrix} x_{se} - x_{sb} & y_{se} - y_{sb} \end{bmatrix}$$

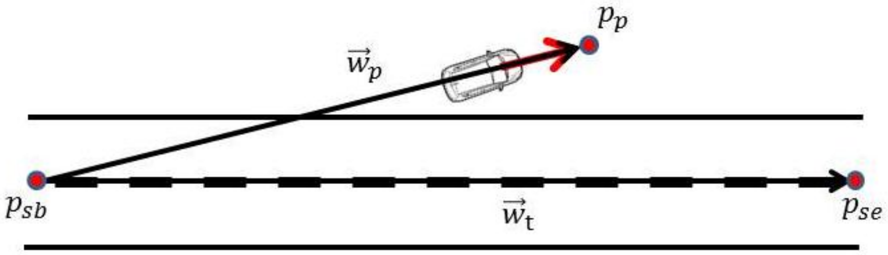

Figure 15. Line segment with vectors $\vec{w}_t$ and $\vec{w}_p$. The vector $\vec{w}_p$ projected onto $\vec{w}_t$ is used to determine whether or not the car is on the current straight segment.

$$\begin{aligned} &(\lambda < 0) && \Rightarrow \text{preview point is before sector} \\ &(0 < \lambda < 1) && \Rightarrow \text{preview point is within sector} \\ &(\lambda > 1) && \Rightarrow \text{preview point is after sector} \end{aligned} \tag{20}$$

Equation 20 determines where the car is relative to the segment. λ is only smaller than zero when the controller is started and the vehicle is before the first segment or if the previous segment was ended prematurely. The controller will therefore not move to the next segment if λ is smaller than zero. If the ratio λ is above one however, the controller will switch to the next segment.

Curved segment

If the current segment is curved it has to be decided whether the preview point is within the corresponding circle sector or not. The sector is defined by the arc starting at the point p_0, ending at p_1 and having the circle centre c_0,(Figure 16 left). To decide whether or not the preview point is within this sector, the vectors $\vec{w}_0$ and $\vec{w}_1$, from the circle centre c_0 to the points p_0 and p_1, and the vector $\vec{w}_p$ between the circle centre and the preview point P_p, are created, see Figure 16. The vectors $\vec{w}_0^{\perp}$ and $\vec{w}_1^{\perp}$, perpendicular to $\vec{w}_0$ and $\vec{w}_1$, are also created.

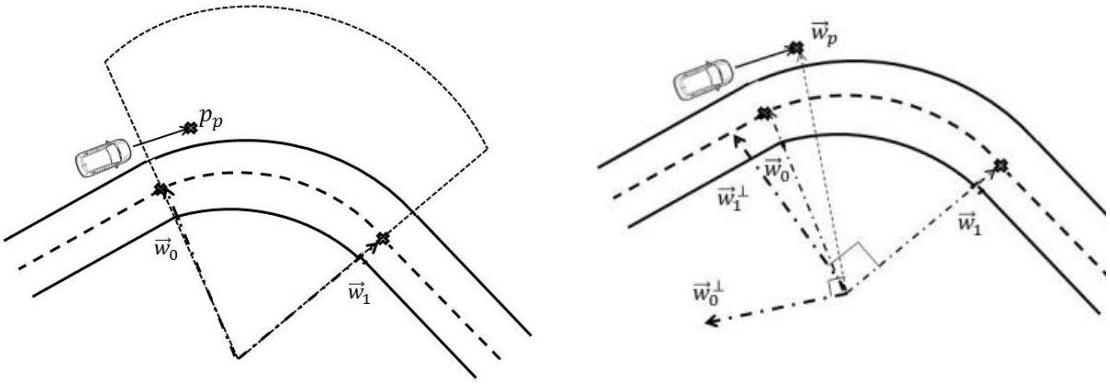

Figure 16: Definition of points (left) and vectors (right) used when checking if preview point is within a segment. Here the preview point is within the curved segment.

Scalar products between the vectors $\vec{w}_0^{\perp}$, $\vec{w}_p$ and $\vec{w}_1^{\perp}$, $\vec{w}_p$ are computed. A geometrical interpretation of these scalar multiplications can be seen in Figure 17.

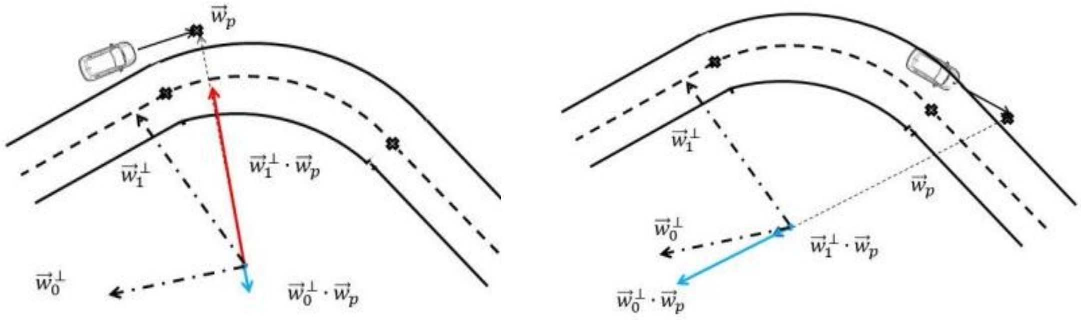
$\vec{w}_p$
$\vec{w}_1^{\perp}$
$\vec{w}_1^{\perp} \cdot \vec{w}_p$
$\vec{w}_0^{\perp}$
$\vec{w}_0^{\perp} \cdot \vec{w}_p$
$\vec{w}_1^{\perp}$
$\vec{w}_p$
$\vec{w}_0^{\perp}$
$\vec{w}_1^{\perp} \cdot \vec{w}_p$
$\vec{w}_0^{\perp} \cdot \vec{w}_p$

Figure 17: Geometrical interpretation of scalar multiplications. In the left figure the preview point is within the sector and in the right it is after the sector.

If these scalar products have unequal signs the preview point is within the current sector. Moreover if the scalar products are both positive and the arc is curved to the right (as in Figure 17) the preview point is before the segment. With both products being negative it can be concluded that the preview point is after the segment (equation 21). The opposite will be true for a left curve.

$$\begin{aligned}
\left(\vec{w}_0^{\perp} \cdot \vec{w}_p > 0\right) \wedge \left(\vec{w}_1^{\perp} \cdot \vec{w}_p > 0\right) &\Rightarrow \text{ preview point is before sector} \\
\left(\vec{w}_0^{\perp} \cdot \vec{w}_p > 0\right) \neq \left(\vec{w}_1^{\perp} \cdot \vec{w}_p > 0\right) &\Rightarrow \text{ preview point is within sector} \\
\left(\vec{w}_0^{\perp} \cdot \vec{w}_p < 0\right) \wedge \left(\vec{w}_1^{\perp} \cdot \vec{w}_p < 0\right) &\Rightarrow \text{ preview point is after sector}
\end{aligned} \tag{21}$$

As with the straight segment no action is taken if the preview point is before the segment but if the point is after the segment the next segment is considered. The vector algebra above is limited to curves less than 90 degrees. Therefore longer curves are split into multiple shorter segments.

4.3 Find nearest point on track

To be able to generate a reference to the controller the preview point is projected onto the track. This is done in different ways depending on the type of segment.

Straight segment

If the current segment is a straight the projection point (x_t, y_t) is calculated using the ratio value (λ) calculated in Equation 19.

$$x_t = \lambda_i(x_{se} - x_{ss}) + x_{ss} \tag{22}$$

$$y_t = \lambda_i(y_{se} - y_{ss}) + y_{ss} \tag{23}$$

Curved segment

If the current segment is an arc the distance from the circle centre (x_0, y_0) is calculated in equation 24. The position of the closest point on the track is calculated in equations 25-26.

$$R_E = \sqrt{\left(x_p - x_0\right)^2 + \left(y_p - y_0\right)^2} \tag{24}$$

$$x_t = \frac{R_t}{R_E}\left(x_p - x_0\right) + x_0 \tag{25}$$

$$y_t = \frac{R_t}{R_E}\left(y_p - y_0\right) + y_0 \tag{26}$$

4.4 Curvature control

To create a reference value to the controller the future path curvature κ that is required to reach a single preview point, Figure 18, is computed.

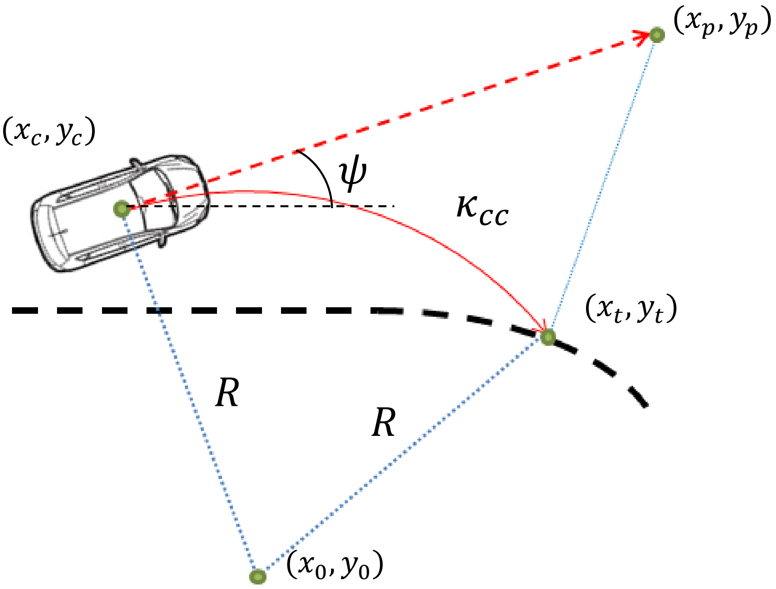

Figure 18. Definition of points used when calculating desired curvature κ_{cc}. The heading angle, ψ, is also for this calculation.

By having information of the current position (x_c,y_c), the preview point on track (x_t,y_t) and the heading angle (ψ) it is possible to calculate the required curve radius. The curved path arc centre (x_0,y_0) is also known from the path definition and lies perpendicular from the vehicle yaw angle at a distance R, equations (27)-(28).

$$x_0 = x_c - R \sin \psi \tag{27}$$

$$y_0 = y_c + R \cos \psi \tag{28}$$

The sign of R will decide whether the arc centre is to the left or right of the heading. Further it is known that the arc centre is also at a distance R from the preview point, giving equation 29.

$$(x_c - x_0)^2 + (y_c - y_0)^2 = (x_t - x_0)^2 + (y_t - y_0)^2 \tag{29}$$

Combining equation 27-29 gives:

$$\kappa = \frac{1}{R} = 2\frac{(x_c - x_t)\sin \Psi - (y_c - y_t)\cos \Psi}{(x_c - x_t)^2 + (y_c - y_t)^2} \tag{30}$$

This controller is a combination of feedback and feed-forward as it calculates a feed-forward gain based on feedback error. The resulting lateral acceleration in the curve given as a reference to the feed forward controller is calculated from the current vehicle speed (equation 31).

$$a_c = \frac{V^2}{R} = V^2\kappa \tag{31}$$

As mentioned in Chapter 2.3, the relation between steering angle and lateral acceleration is highly non-linear for most vehicles. To be able to determine the steering angle needed to follow a desired curvature the relationship between lateral acceleration and hand wheel angle is needed. How this is determined is presented in the following chapter.

4.5 Mapping of steering angle

To generate a steering angle control signal from the preview curvature a function from desired curvature to steering angle is required. This function is generated from driving in a circle with low acceleration until the limit of adhesion. The measured steering wheel angle from a manually driven steady state circle manoeuvre is plotted versus the resulting lateral acceleration. A curve fit is performed to approximate this relationship with an exponential function, see equation 32. When using the function the future lateral acceleration is approximated from the curvature calculated in chapter 4.4 and current vehicle speed.

If the radius, and hence curvature is kept constant equation 32 becomes a function of only vehicle speed. As the curvature is changed the Ackerman steering angle offsets the curve while the linear and non-linear behaviour is almost constant. As seen in Figure 19 this gives a good approximation of the real behaviour. The calibration constants for three vehicles are given in Table 4 and are related to the vehicle's steering behaviour as:

$$\delta_{ss} = \kappa(K_a L + K_l V_x^2) + K_e e^{(\kappa V_x^2 - A)} - K_e e^{(-A)} \tag{32}$$

K_a: Steering ratio calculated from simulation.
K_l: Gradient of the linear handling region.
K_e: Gain for non-linear region.
A: Start value (lateral acceleration) for non-linear region.

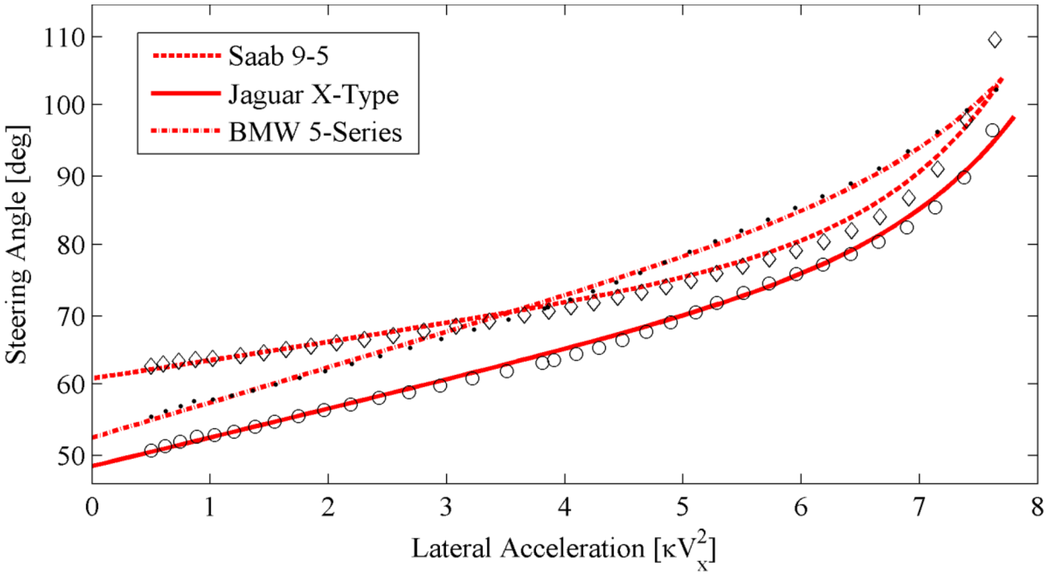

Figure 19. Curve fit of a Saab 9-5, BMW 5-series and Jaguar X-type, Sampled lines are measurement data. Constant *κ*.

Table 4. Calibration constants from steady state circle driving.

	K_a	K_l	K_e	A
Saab 9-5	15.73	0.046	0.031	5.09
BMW 5-series	13.53	0.088	0.042	6.00
Jaguar X-Type	12.47	0.072	0.058	6.08

The controller is often used for transient manoeuvres were the steady state steering angle is not sufficient to describe how the vehicle will yaw and accelerate. To compensate for response delay the control inputs are performed earlier than would be needed if driving in steady state. This is done by letting the controller believe that the vehicle is at an advanced position in the heading direction, compared to actual position. A suitable advancement time, called t_{step}, is around half of the average response time presented in Table 1.

4.6 Angular error feedback

By adding feedback information of deviation from the current track angle extra functions for vehicle stability can be implemented in the controller. Currently the angular feedback is used to compute the correct driving direction. This enables the vehicle to return to the track in the correct direction even after large deviations.

For straights the angle is of course constant for the entire segment but for curves the current angle has to be updated as the vehicle drives along the arc. Equation 33 calculates the angle change since the starting point of the arc and equation 34 calculates the track angle, φ_s is the starting angle of the current segment. If the angular error φ_E becomes too large (above 90°) the curvature control deactivates and vehicle is returned to the correct direction by the angular feedback control. When the error is well below 90° the curvature control reactivates.

$$|\varphi_d| = \mathrm{acos}\left(\frac{\vec{w}_c \cdot \vec{w}_0}{|\vec{w}_c||\vec{w}_0|}\right) \tag{33}$$

$$\varphi_t = \varphi_s + \varphi_d \frac{\kappa_i}{|\kappa_i|} \tag{34}$$

$$\varphi_E = \varphi_t - \psi \tag{35}$$

5 Control of specific manoeuvres

The *Preview Curvature Controller* is developed for track following. To manage the more specific manoeuvres presented in the goal statement individual modifications are done to the controller. The three modifications are presented in this section.

5.1 Steady state cornering controller

When performing a steady state circular driving manoeuvre (chapter 2.4.4) the required steering wheel angle will slowly change as the lateral acceleration of the vehicle increases. For most standard cars the change will be an increase due to understeer. At low speeds however the hand wheel angle needed to follow a curved path is dependent only of the wheelbase, corner radius and steering ratio according to equation 36. Using this relationship as a starting point, a feed forward controller can be specified as

$$\delta_{hw} = \frac{L}{R_t} i_s \tag{36}$$

where i_s is the overall steering ratio and *r* is the radius of the circle. This relationship is the same as in equation 5 but with K_{us} set to zero.

Using the *Preview Curvature Controller* when the car is currently on the reference track curvature at low speed will result in the same steering wheel angle as in equation 36, given that the steering ratio K_a in equation 32 is correct. When the speed starts to increase the other coefficients in equation 32 will of course also affect the steering wheel angle.

As the speed increases the vehicle will start to slowly drift away from the set radius, even with a perfect tuning of steering wheel angle versus lateral acceleration. This is due to the delay between a change in hand wheel angle and the resulting change in lateral acceleration of the car. With a poor tuning of the controller or changes in surface conditions the deviation from the path will of course become larger.

To limit this deviation, a pure I-controller which uses the current error, i.e. no preview, in distance from the centre of the circle as input, has been added in cascade with the *Preview Curvature Controller*.

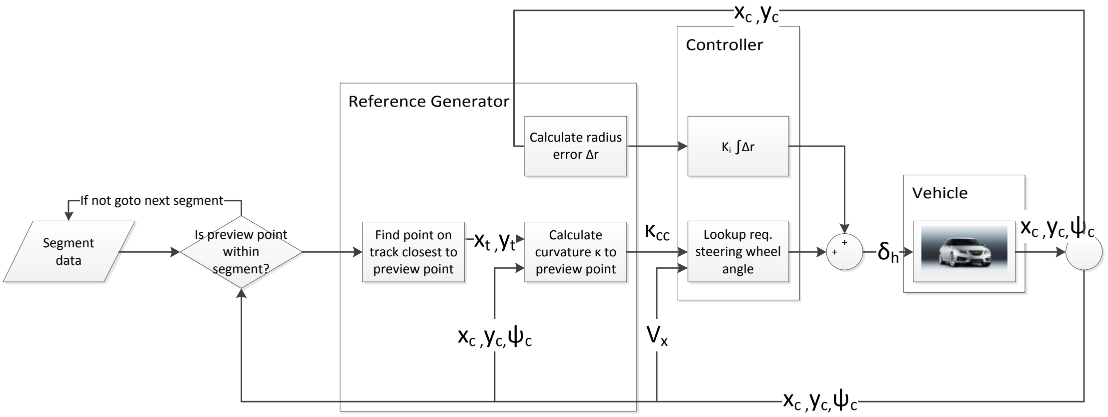

x_c, y_c
Controller
Reference Generator
Calculate radius error Δr
K_i ∫Δr
Vehicle
If not goto next segment
Segment data
Is preview point within segment?
Find point on track closest to preview point
x_t, y_t
Calculate curvature κ to preview point
κ_cc
Lookup req. steering wheel angle
+
+
δ_h
x_c, y_c, ψ_c
x_c, y_c, ψ_c
V_x
x_c, y_c, ψ_c

Figure 20: The controller structure when extended with integral action on the radius error.

The radius error when using the controller can be seen in Figure 21. The highest integrator gain ($K_i = 0.01$) in the figure is the highest gain that does not make the vehicle unstable. Anti-windup (see chapter 2.5.3) has also been added to stop the integration when the steering angle output at a maximal allowed level.

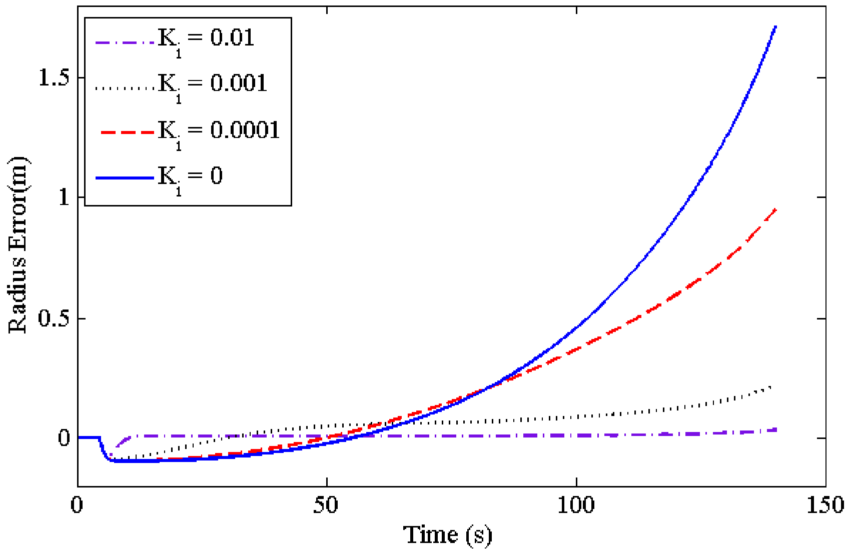

Figure 21: Radius error over time for different integrator gains (*K_i*). Further increasing the gain causes the steering to oscillate. Only an approximated value of the steering gain an wheel base is used for the proportional preview gain.

5.2 Track limit observer

The track limit observer is used to ensure that the vehicle does not run off the track during an open loop manoeuvre. If the car approaches the track boundary to fast the manoeuvre is aborted and the car is positioned along the edge of the track. It is assumed that open loop manoeuvres will be performed at straight track sections where it is easy to define the track limits on the left and right side of the car. For the purpose of the thesis the sine with dwell manoeuvre is used to evaluate the track limit observer. During an open loop manoeuvre the distance to the track boundary and the vehicle yaw angle is constantly observed. This data is used to calculate which path curvature is required for the car to touch the track limit, see Figure 22 and equation 37. Assuming constant speed the equivalent lateral acceleration is calculated, equation 31. Before the manoeuvre is started a threshold is set for lateral acceleration. If the anticipated lateral acceleration exceeds this value the open loop manoeuvre is stopped and the car returns to the starting point of the manoeuvre.

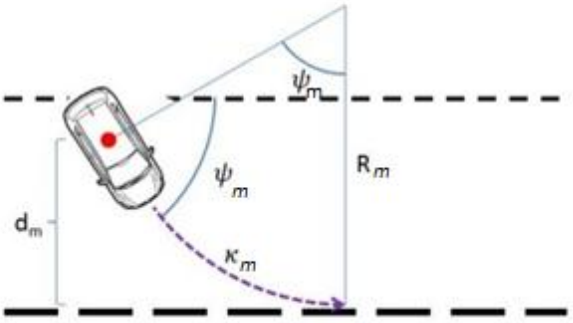

Figure 22. Track limit observer.

$$\kappa_m = \frac{1}{R_m} = \frac{1-\cos\psi_\mathrm{m}}{d_m} \tag{37}$$

5.3 Sine sweep manoeuvre

During a sine sweep the steering wheel is moved in a sinusoidal movement with linearly increasing frequency, typically 0.2 to 4 Hz, equation 38.

$$\delta = k\sin\left[2\pi t\left(f_0 + \frac{k_c}{2}t\right)\right] \tag{38}$$

where f_0 is the initial frequency, k_c is the rate at which the frequency increases.

A sine signal will give the car an average heading angle proportional to the amplitude towards the initial steering direction. Integration of the yaw rate gives a yaw angle which varies only above or below the initial yaw angle, equation 42. The steering angle required to follow a curve with radius R for a time independent vehicle model is:

$$\delta = \frac{L}{R} \tag{39}$$

The yaw rate is defined as:

$$\Omega = \frac{V_x}{R} \tag{40}$$

Expressing the yaw rate as a function of δ, assuming constant speed V_x, and integrating over time gives equation 41. Setting the steering input to be a sine wave signal with angular frequency f and amplitude a gives equation 42, where $(\cos 2\pi f t - 1)$ varies between -1 to 0.

$$\int_0^T \Omega\, dt = \int_0^t \frac{V_x}{L/_{\delta}}\, dt \tag{41}$$

$$\delta = a\sin 2\pi f t \Longrightarrow$$
$$\psi = -\frac{V_x}{L}\left(\frac{a}{f}(\cos 2\pi f t - 1)\right), \qquad t \in 0, \infty \tag{42}$$

An initial steering input is given before the original sine sweep to make the yaw angle to vary around the centre line of the track. The initial compensating steering signal should be opposite and half of the original sine giving:

$$\delta_{init} = -\frac{a}{2}\sin 2\pi f t \quad , t \in 0, \frac{1}{2f} \tag{43}$$

Adding δ_{init} to the manoeuvre gives:

$$\psi = -\frac{V_x}{L}\left(\frac{a}{f}(\cos 2\pi f t - 1) + \frac{a}{2f}\right) \tag{44}$$

$$-\frac{V_x}{L}\frac{a}{2f} \leq \psi \leq \frac{V_x}{L}\frac{a}{2f} \quad , \qquad t \in -\infty, \infty \tag{45}$$

The frequency of the initial steering compensation is set equal to the initial sine sweep frequency since this determines the yaw bias. When integrating a chirp signal the bias of the signal is slowly growing. However, the bias rapidly approaches a constant value and this is why the frequency can be set constant for the initial compensation.

External disturbances such as wind, uneven tracks and friction variations also affect the mean heading during the manoeuvre. To keep the car on the track a feedback controller is implemented to compensate for disturbances. The frequency content of the signal should be altered as little as possible while maintaining this heading. To minimise the feedback influence the feedback gain is very low and no correction is made until a predetermined distance from the centre line. The open loop steering angle δ_{open} is compensated according to equation 46 using current car position and one preview point:

$$\delta = \delta_{open} - k_1(|y_c| - y_{lim})\frac{|y_c|}{y_c} - k_2(|y_p| - y_{lim})\frac{|y_p|}{y_p} \tag{46}$$

where y_{lim} is the threshold at which the feedback activates, y_c is the car’s distance from the centre line and y_p is the preview point’s distance from the centre line.

6 Implementation of controller

The *Preview Curvature Controller* has been implemented in the real time computer controlling the robot from Vehico. This chapter describes the hardware installed in the vehicle and important considerations when combining the new controller with existing open loop control.

6.1 Installation in vehicle

The subsystems installed in the vehicle are the following:

- Real-time computer and power electronics unit (see chapter 2.1)
- Steering actuator (see chapter 2.1)
- VBoxIII 100Hz GPS receiver and antenna(see chapter 2.2.1)
- iMar FMS Inertial measurement unit (see chapter 2.2.2)
- Additional 12V battery

The additional power supply is needed only to prevent the IMU from rebooting, hence demanding a recalibration, when starting the engine or when the steering actuator is drawing high currents. The real-time computer has an onboard battery to prevent it from rebooting at voltage drops.

The two measurement systems communicate with the real-time computer over two separate CAN busses.

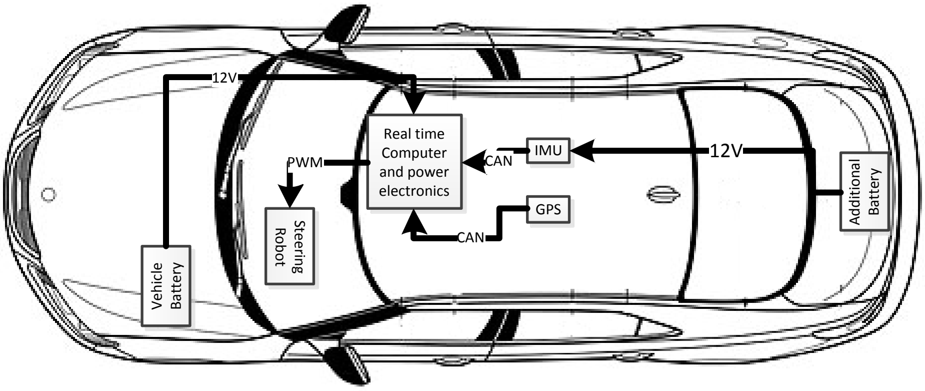

Figure 23: Location of subsystems in the vehicle

6.2 Coding

This section describes how the *Preview Curvature Controller* is implemented into the real-time computer controlling the steering robot.

The implementation has been done so that the new commands, `DriveStraightLine` and `DriveCurve`, are compatible to the existing open loop commands. It has also been taken into account that the new controller shall fit into the framework of the original control software of the Vehico Robot.

The controller reads in one track segment at a time to enable combinations of open loop and closed loop commands. When the vehicle leaves one segment the controller is given the information about the following segment.

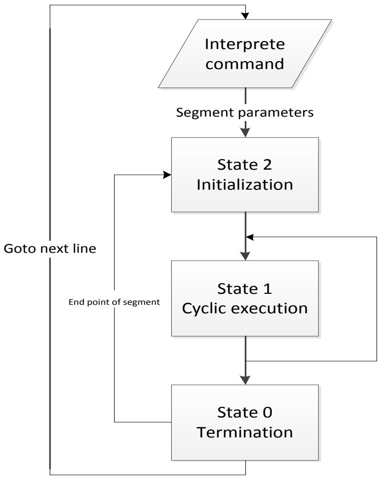

Figure 24. The structure of the implemented controller.

The structure of the controller is described in Figure 24. The framework used with the three states is the same as for open loop commands. The execution is started when the command interpreter reads in a closed loop command and its parameters. State 2 initializes the command by performing calculations that are not required in every iteration. This is done to make the cyclic execution in state 1 faster.

With the initialization done the cyclic execution of the reference generator and controller is started. The cyclic execution takes the following steps:

1. Read in data from shared memory, including vehicle position, speed and accelerations.
2. Calculate the preview distance.
3. Calculate the location of the preview point.
4. Calculate vectors to check if preview point is on segment (section 4.2). When the segment is passed, break and go to state 0.
5. Calculate the reference feed forward curvature.
6. Apply control law to the reference.
7. Check for saturation
8. Update shared memory with control output (desired steering angle).
9. Return to 1.

When the controller considers the segment to be finished the execution moves into state 0. In this state the startpoint and angle of the next segment is set to the endpoint and ending angle of the current segment.

The cyclic execution described here is one of many real time tasks running on the real time computer. One of the other tasks converts the desired steering angle to a physical control signal which is sent to the drive electronics.

6.3 Kinematic Kalman filter implementation

To get a smoother position reference signal a discrete kinematic Kalman filter (chapter 2.2.3) was implemented. The filter runs at the same sample rate as the controller, 500 Hz. Currently the Kalman filter runs within the same real-time task as the controller, but it is recommended that it is moved into a separate task so the timing can be controlled more accurately.

The measured data from the GPS and inertial measurement system is sampled at 100 Hz. The parameters R_1 and R_2 (see chapter 2.2.3) determines how the inertial measures are weighted versus the GPS measurements were tuned in the test vehicle. It was found that increasing the weight on the inertial measurements (lowering the value of R_1) increased the delay introduced by the filter. The effects of changing the weights can be seen in Figure 25. The weights from the rightmost of the plots in Figure 25 are used in the implemented filter, meaning that a much higher emphasis is put on the GPS measurements. In a sharp turn as in Figure 25 the offset between measured GPS and filtered position is at most 0.15 meters with the used values on R_1 and R_2.

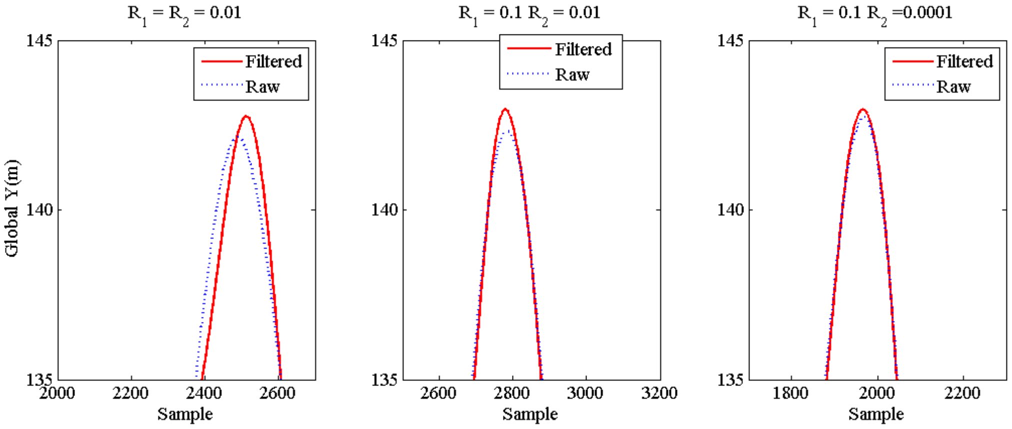

Figure 25: Effect of changing the weighting between inertial measurements and GPS measurements. Increasing R_1 decrease the influence of the inertial measurements on the filter output and increasing R_2 decrease the influence of GPS measurements. Only the relative weight of R_1 versus R_2 is of interest. The filter is updated every 0.002 seconds.

6.4 Safety functions

As a failure of the system can lead to a faulty steering wheel output that might cause the vehicle to run of track, functions that mitigate the effect of a failure were implemented.

To increase the reliability of the data acquisition a safety function was implemented so that almost no emphasis is put on the GPS measurements if the number of satellites in view is too low or if the GPS system would fail. In case of a failure of the GPS system the position would soon become faulty but the safety function gives the operator a chance to abort the test in a controlled manner.

As the weight of the GPS measures in normal operation is high a failure of the inertial measurement system would not greatly affect the output of the filter. The operator would be able to abort the test in a controlled way without changing the filter parameters.

The IMU provides the controller also with the vehicle yaw angle. If the system ceases to function the signal to the controller becomes zero. This leads to a preview point in the wrong direction, and consequently a large steering output. To avoid this problem a function has been implemented which makes the controller use the heading angle from the GPS if the IMU fails.

7 Simulation Results

This chapter presents the results from simulations of track driving and the control of specific manoeuvres.

7.1 Track driving results

The trackdriving simulations in IPG CarMaker has been performed on the Hockenheim track using IPG driver for longitudinal control.

7.1.1 Effect of preview time on precision versus stability

Once the *Preview Curvature Controller* has been calibrated (Chapter 4.5) the only tuning parameter is the preview time. The resulting reference curvature calculated as described in chapter 4.4 becomes larger as preview time is decreased. The track curvature changes in steps, because lines and arcs are used to define the track, meaning that a short preview time will lead to a rapid change in the desired curvature. A long preview will hence lead to a smoother controller, but also to a larger corner cutting and larger deviations from the reference track, see Figure 32. The user has to make the trade-off between precision and smoothness.

Simulations have been made to determine appropriate values for the preview time. As the velocity of the car will be controlled by a human driver when testing the controller in a vehicle IPG Driver was used for longitudinal control in simulations. As IPG driver is completely decoupled from the steering controller it will not perform very well, meaning that the car might be braking or accelerating while turning and thereby destabilizing the vehicle. This is not completely undesirable as stability must be guaranteed also with such disturbances. The destabilizing behaviour can also be avoided by lowering the acceleration limits in IPG driver resulting in more careful driving in curves.

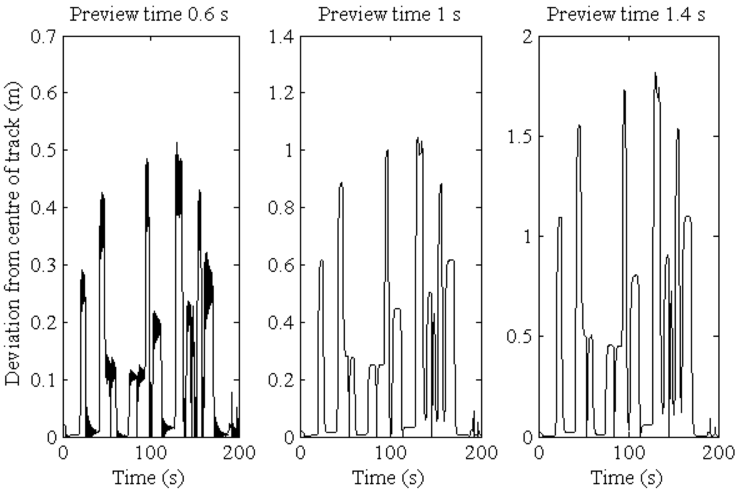

Figure 26: Deviation from centre of track versus time. Notice the difference in the scale of the y axis, the deviation from the centreline is approximately 4 times larger with the longest preview time compared to the shortest. IPG driver is set to drive at constant speed, 50 km/h.

Figure 26 shows the effect of changing the preview time on deviation from the centre line of the track. With 0.6 seconds preview time the controller is oscillating around the reference path, seen in Figure 26 and Figure 28. Figure 27 shows how the mean deviation from the centreline increases with preview time.

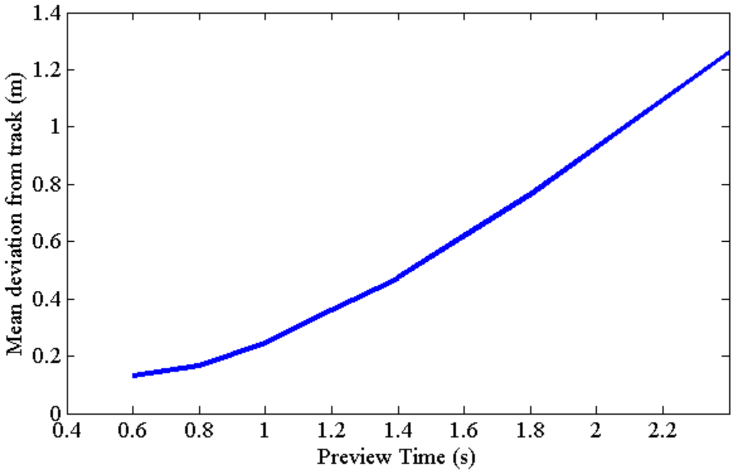

Figure 27:Mean deviation from track centre line at different preview times. The mean deviation increases almost linearly with preview time.

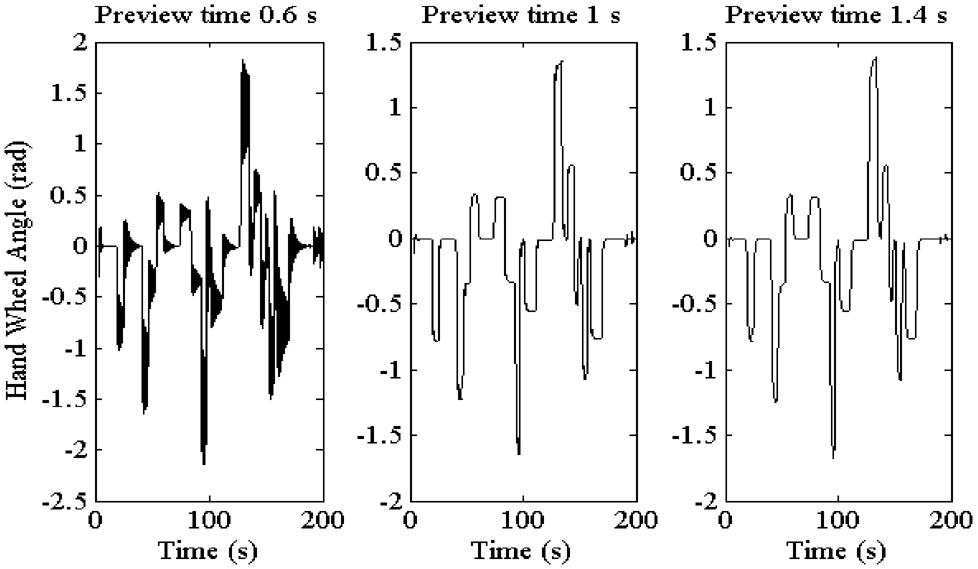

Figure 28: Steering angle over time for different preview times. At 0.6 seconds preview time the steering wheel oscillates considerably.

From the simulation results shown in the figures 26-28 it was decided that a preview time of 0.8 seconds gave a good path following performance without excessive control signal activity.

7.1.2 Precision, from straight segment to curve

The car was driven at a track starting with a straight segment, entering a 180° turn and finishing with a straight segment. This was done to visualize the positional precision of the controller and investigate how different settings affect the precision. Since the control input comes solely from one preview point absolute precision is not achievable, neither is it a strong demand on the controller. However, it is still of interest to evaluate the precision and how it can be improved if future use demands a higher precision.

In the first experimental set the car is driven in five different curves with different radius. The speed is set so that the lateral acceleration will be 2 m/s^2 in each run. Decreasing radius means that the error increases and the car travels on the inside of the specified curve. However, even in the tight 20 meter radius bend the error does not exceed 0.5 meters. As mentioned above it is expected that perfect tracking is not possible in tight bends because preview is the only feedback source.

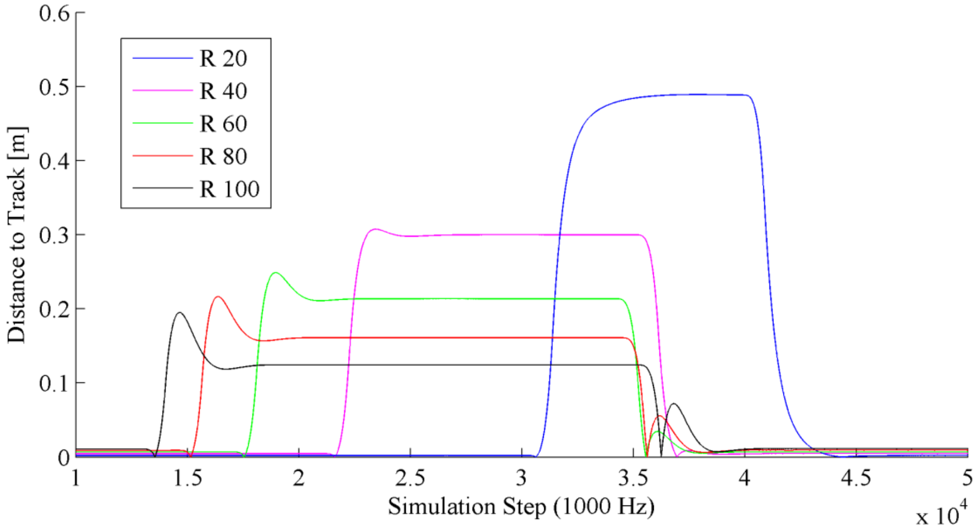

Figure 29. Positional error with varied curve radius, constant lateral acceleration of 2 m/s^2.

In the second experiment the same set of curves is driven but with a constant speed of 30 km/h. The results are very similar to the first experiment showing that the accuracy is similar even if the speed is different. It can in Figure 29 be seen that the higher velocities reached in experiment 1 causes overshoot when entering and exiting the curve.

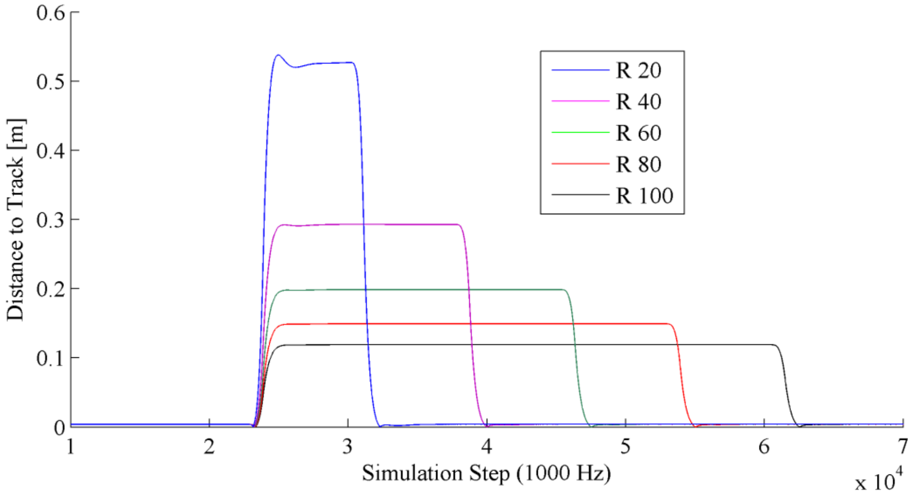

Figure 30. Positional error with varied curve radius. Velocity 30 km/h.

The third experiment involved changing the response parameter t_{step}. The vehicle position information is advanced compared to the real position to make the controller turn the car earlier. The car was driven at either 100 or 60 km/h in a 100 meter radius bend. At 60 km/h the best results are achieved when no response compensation is made though at higher speeds it is necessary if the vehicle should be kept within one meter from the track. This happens because the delay in lateral acceleration causes the vehicle to turn to late. To achieve high precision both for low and high speed the response parameter was set to vary with speed. This approach gave good results and, except from some overshoot, the error kept within 0.5 meter for lateral accelerations from 0.7 to 7.7 m/s^2.

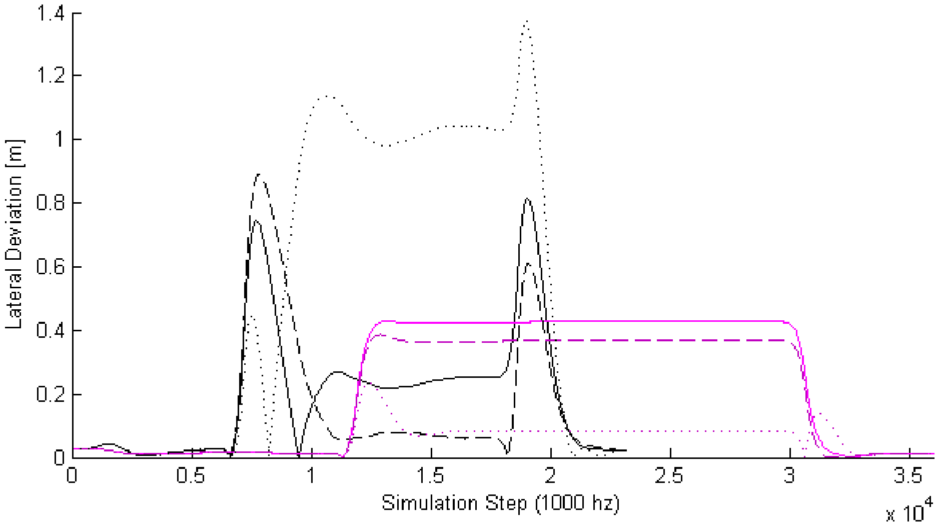

Figure 31. Positional error in R100 curve. Black = 100 km/h, purple = 60 km/h. Solid lines – t_{step} = 0.1, dashed lines – t_{step} = 0.005V, dotted lines – t_{step} = 0.

The precision experiment shows that the design of controller and steering map are successful in giving good tracking performance with a very simple and fast calibration manoeuvre. Only three settings for response compensation were tried so this would be a source of improving the precision by developing a more advanced dependency on velocity or lateral acceleration. Figure 32 gives an explanation to why the controller cuts the corners. Since the preview point enters the curve before the vehicle does the preview curvature will cut the corner with a large radius starting before the track bend begins.

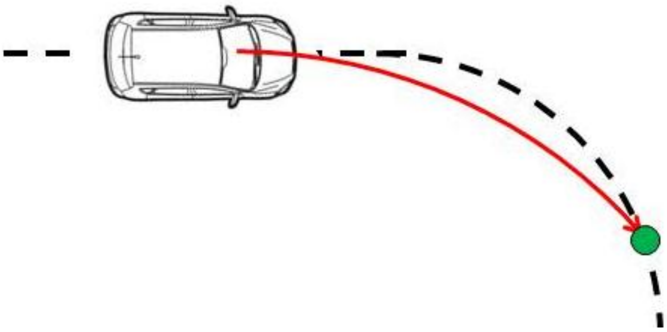

Figure 32. Corner cutting because of preview.

7.1.3 Robustness

To verify that the controller is able to handle disturbances such as changing friction, unexpected brake input and sudden changes in the reference signal several tests have been performed in simulations. These tests have all been performed in the same 19 meter radius curve. The corner is followed by a short 20 meter straight and then, to make the manoeuvre more difficult, another curve with radius 25 meters. The track section used can be seen in Figure 33.

Besides these specific tests the controller has shown to cope well with disturbances such as acceleration and breaking while turning. Because the longitudinal controller of IPG CarMaker is decoupled from the *Preview Curvature Controller* this acceleration and breaking appears as an undesired disturbance. However, the ability to cope with this disturbance is a measure of how robust the controller is.

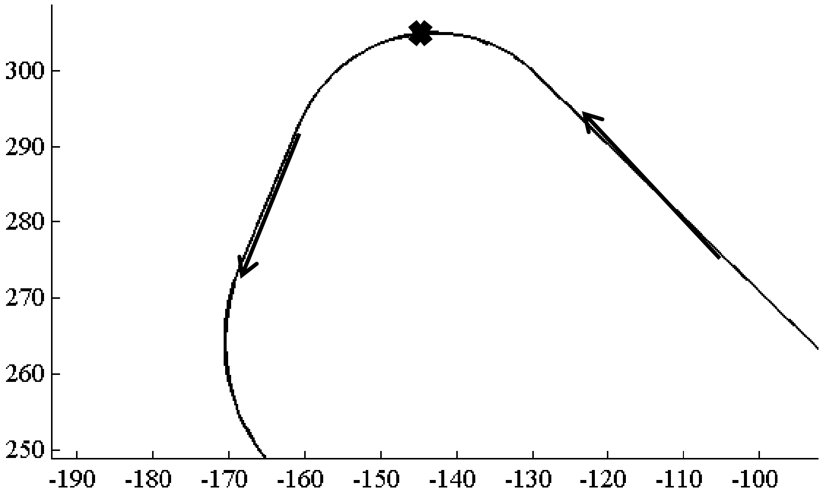

Figure 33: The track section used for evaluation of robustness. The point where the disturbances were applied is marked with an x.

Friction change

The effect of a step change in friction was studied while the vehicle was in the first corner of the track section in Figure 33, with a constant speed of 30 km/h. The friction was lowered in the middle of the corner. It was shown that as long as the tyres can generate enough side force the controller performance remains close to in the undisturbed case.

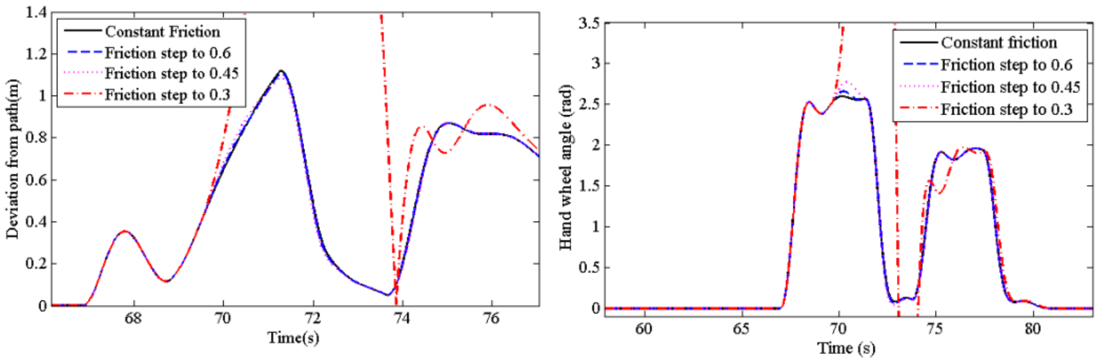

Figure 34: Result of a friction change while cornering. The deviation from the centreline of the path(left) remains unchanged as long as the tires can generate enough side force.

Braking the rear wheels

To evaluate how the controller can cope with oversteer a test has been performed in which the rear wheel are braked while the vehicle is in a tight curve. The speed of the front wheel driven car is set to a constant 40 km/h and the longitudinal controller tries to keep this speed even when braking the rear wheels.

In Figure 35 it can be seen that applying the rear brakes during cornering after 51 seconds causes sudden yaw acceleration. Both when braking the wheels for 0.5 and 1 second the vehicle becomes stable before exiting the track section seen in Figure 33.

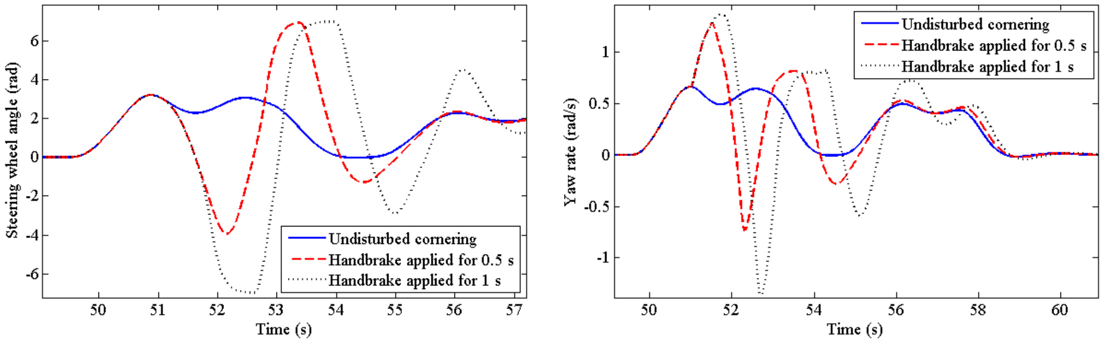

Figure 35:The impact of disturbing the vehicle by applying brake torque on the rear wheels.

Position signal step

Because the signal from the GPS system might be subject to step disturbances as one or many of the satellite signals is not received, the effect of a step disturbance while cornering was studied. The car has a velocity of 40 km/h in the test and is on the section shown in Figure 33.

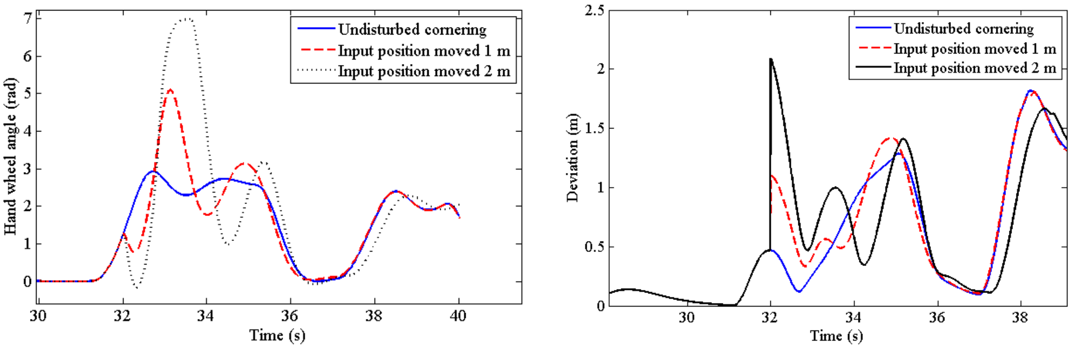

Figure 36: The effect of a step in the position signal while cornering. The lateral and longitudinal signal is moved one or two metres each.

7.2 Steady state circle results

The cascaded steady state cornering controller introduced in section 5.1 has been tuned and evaluated only in simulations. The reason for only evaluating the controller in simulations was the lack of access to a large enough vehicle handling area to perform the steady state cornering manoeuvre. However, the resulting gain schedule for required steering gain generated from the steady state cornering simulations have been used with good result when evaluating the track driving controller. The performance of the steady state circle controller is shown in Figure 21.

7.3 Results of superimposed control of open loop

The superimposed feedback control in open loop manoeuvres were evaluated in a sine sweep manoeuvre and a sine with dwell manoeuvre. The track limit observer described in chapter 5.2 successfully aborts the manoeuvre if the boundary approaches faster than the threshold lateral acceleration allows. An analysis of the influence on the sine sweep manoeuvre is presented below.

A sine sweep manoeuvre from 0.1 to 4 Hz with an increase of 0.1 Hz/s was performed to evaluate the influence of feedback control. The controller is activated at four meters from the centre line and uses two preview points 1 and 2 seconds ahead of the car. To increase the deviation from the centre line the track had a camber angle of 10%. As seen in Figure 37 the feedback control successfully maintains the car along the centre of the track. Figure 38 shows the frequency content of the steering input estimated using the function *pwelch* in Matlab. As can be seen the frequency content is very similar with and without closed loop control with only a slight shift in gain.

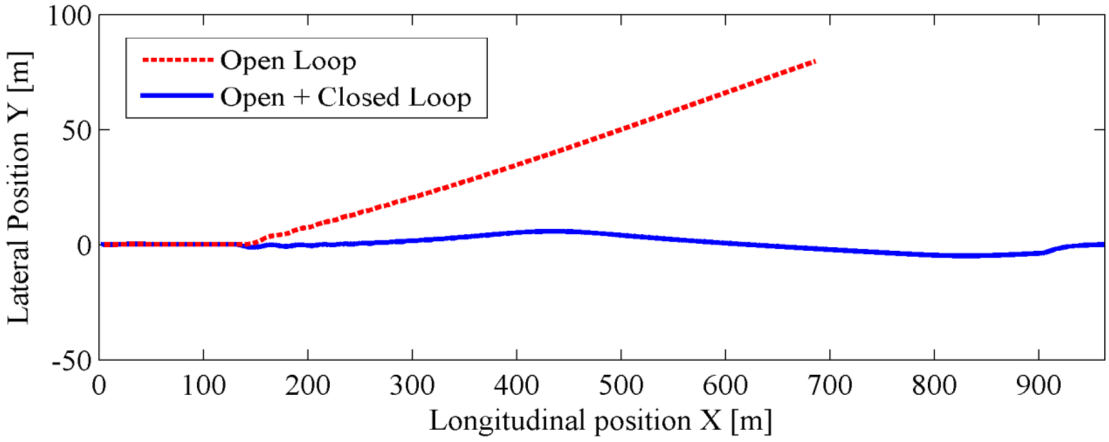

Figure 37. Deviation from centre line during sine sweep. The superimposed closed loop control manages to keep the vehicle close to the centre of the track despite the large camber angle.

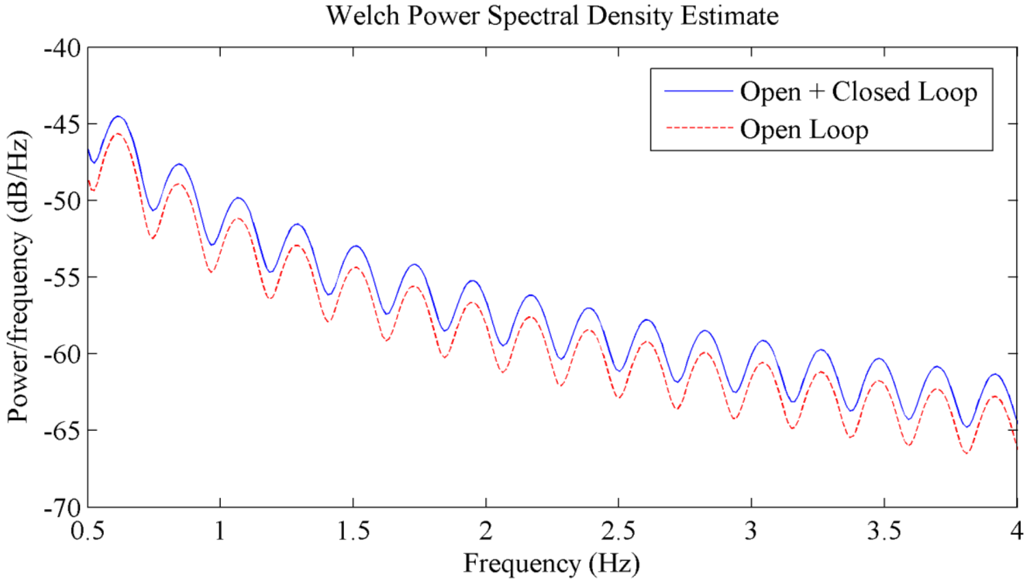

Figure 38. Power spectral density of steering wheel input during sine sweep. The closed loop control has very little effect on the frequency content.

Figure 39 and Figure 40 shows bode plots of the transfer function estimates, done with Matlab function *tfestime*, from steering angle to lateral acceleration and yaw rate respectively. As seen these show very good agreement with only a slight deviation in gain for the yaw rate at frequencies lower than 0.4 Hz which is below the range of interest. The closed loop control keeps the car within 10 meters from the centre line and since the effect on the frequency analysis is small this should be a useful tool when performing a sine sweep on a narrow track.

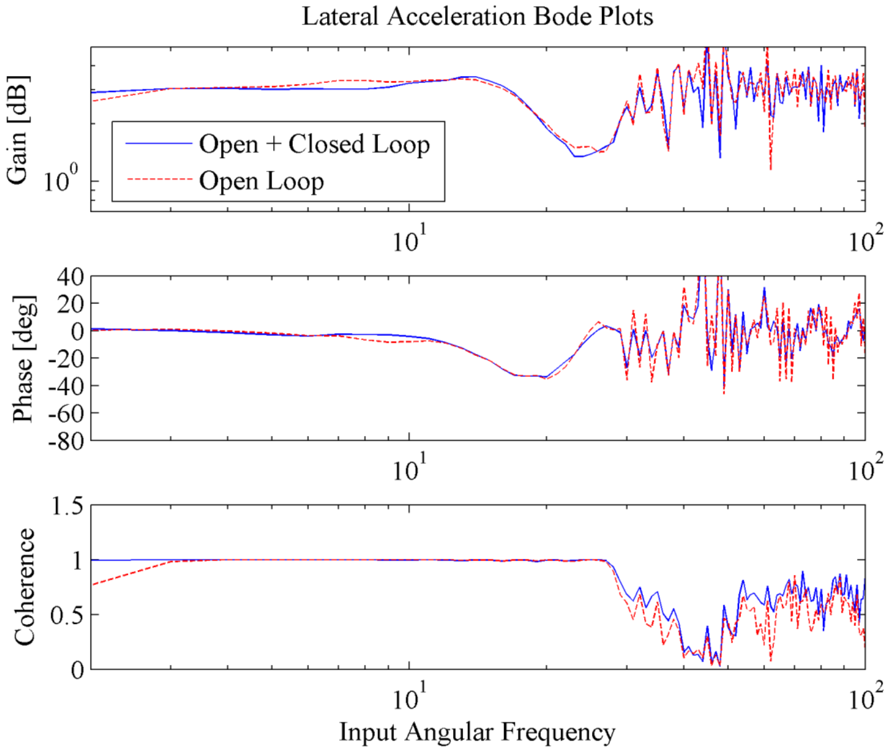

Figure 39. Lateral acceleration response during sine sweep. The plots show a very good coherence with and without the feedback control.

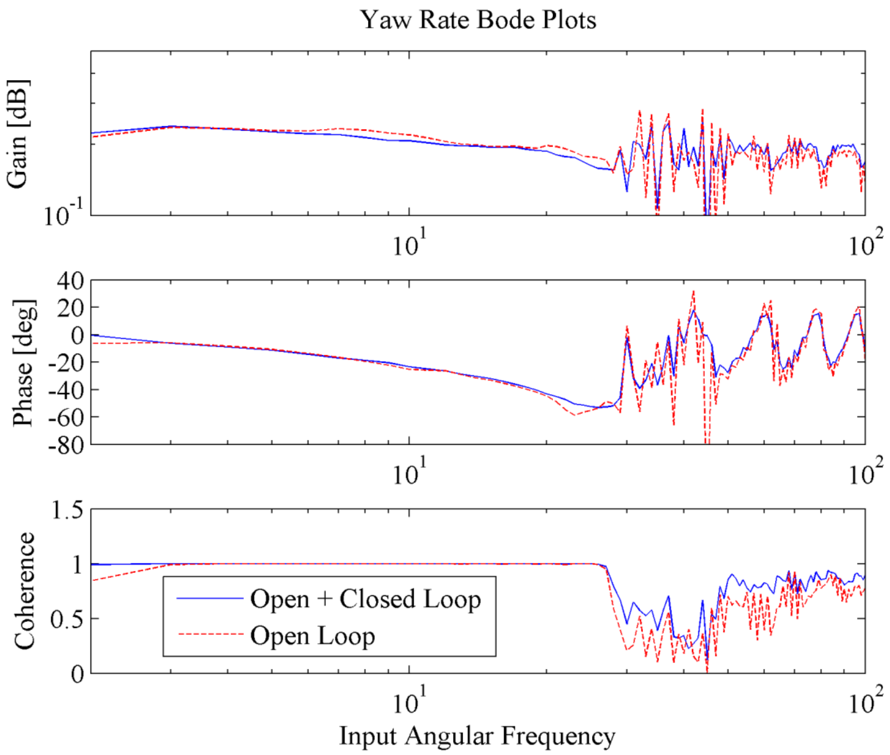

Figure 40. Yaw Rate response during sine sweep. The plots show a very good coherence with and without the feedback control.

8 Physical testing results

The physical testing of the controller has been made at a decommissioned air field used by, among others, SAAB to perform vehicle testing. The airfield suits the needs for the evaluation of the controller as it is on an open field, hence less disturbances to the GPS signal. Because there is only grass on the side of the road the risks in the event of a controller failure are small.

Compared to the Hockenheim track used in most of the simulations the track at Råda airfield is shorter and narrower, Figure 42. It has a long straight, a couple of narrow turns and a large radius curve to enable evaluation of the controller performance in all these situations.

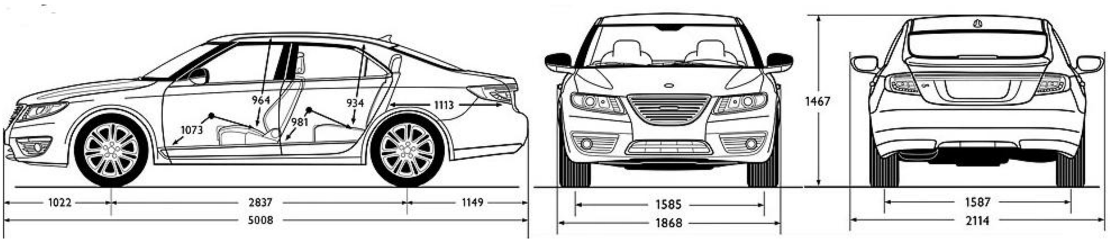

Figure 41:The SAAB 95 used when validating the controller.

The vehicle used in the validation is a four wheel driven SAAB 9-5 sedan with a 190 Hp diesel engine. The 9-5 is a very stable car yet reasonably agile for its weight of approximately 2000 kg.

The preview time used in all physical tests is 0.8 seconds. On top of that a smallest preview distance of 10 meters has been used to limit the hand wheel angles at low speed.

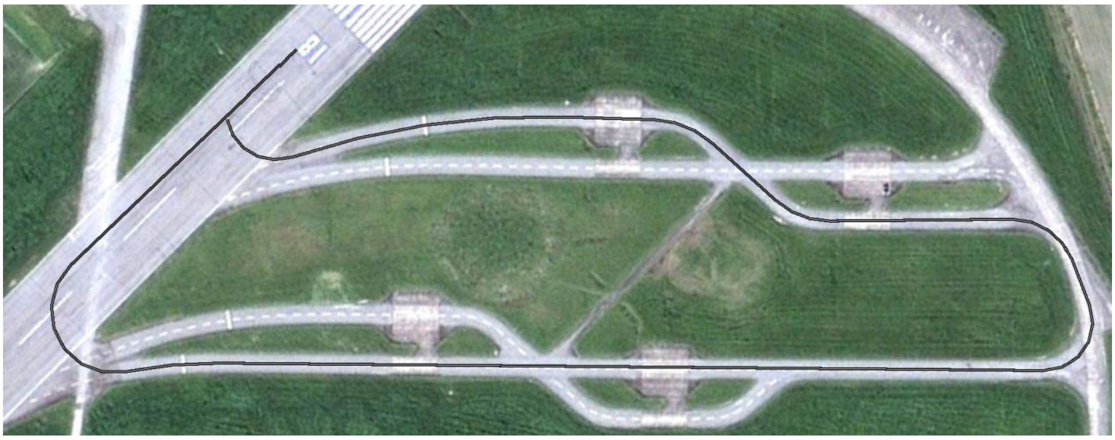

Figure 42: The track driven at Råda airfield.

8.1 Precision

The precision of the controller is shown to be very high when on straights. In Figure 43 the deviation on the long straight (from 15 to 25 seconds) is below 0.1 metres. When cornering the preview cause the car to cut the corners (Figure 44). However, the vehicle still stays within 1.2 metres from the centreline of the track at all times. In longer bends, as the one opposite to the long straight in Figure 42 the deviation from the centreline decreases over time, as seen in Figure 43 (between approx. 53 to 57 seconds).

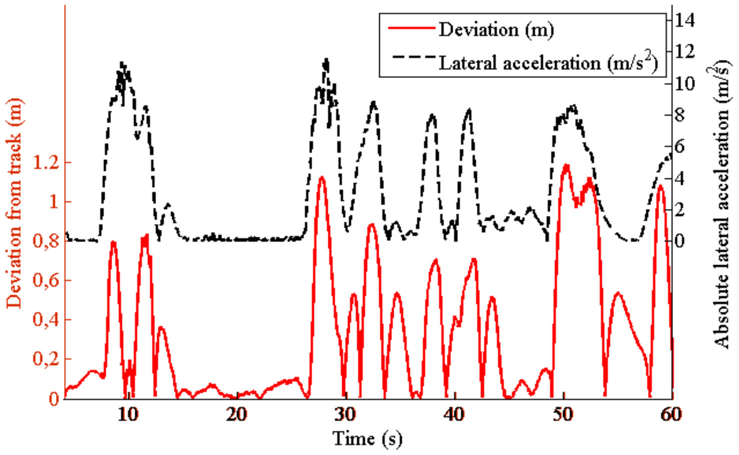

Figure 43:The deviation from the track during one lap of the Råda track. The deviation is here related to the lateral acceleration of the vehicle. The speed was high, exceeding 100 km/h on the straight. The speed was kept high enough to reach lateral accelerations of 8-10 m/s^2 in all bends.

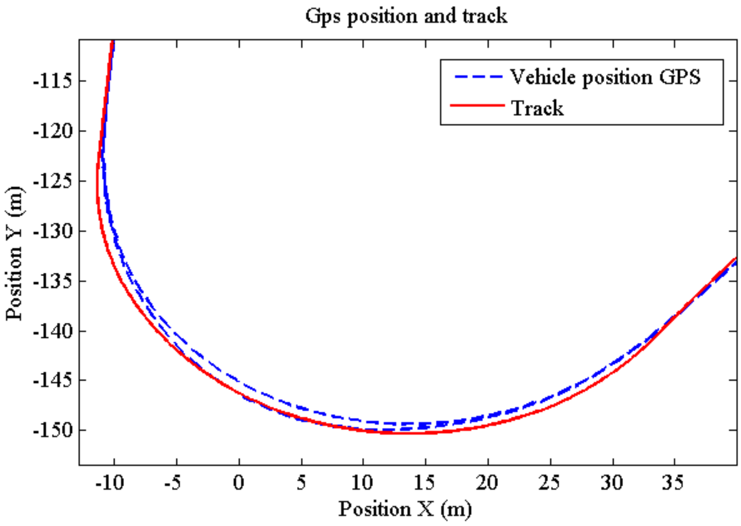

Figure 44: Vehicle position relative to the track when cornering at high speed. The lateral acceleration of the vehicle is between 0.8 and 1 g. Preview time is 0.8 seconds, with a minimum preview distance of 15 meters. The difference in path is due to different speeds, the path closest to the track is driven at highest speed with the front tyres entering saturation.

8.2 Control signal activity

The control signal has proven to be very smooth during the physical testing. In Figure 45 the control signal from the same lap around the Råda track from which the data presented in Figure 43 was recorded, is shown. In the right plot of Figure 45 the small delay between requested hand wheel angle and actual hand wheel angle can be seen.

As seen in the left plot of Figure 45 the control signal is smooth and the mechanics of the actuator can in the right close up be seen to filter out the noise in the control signal.

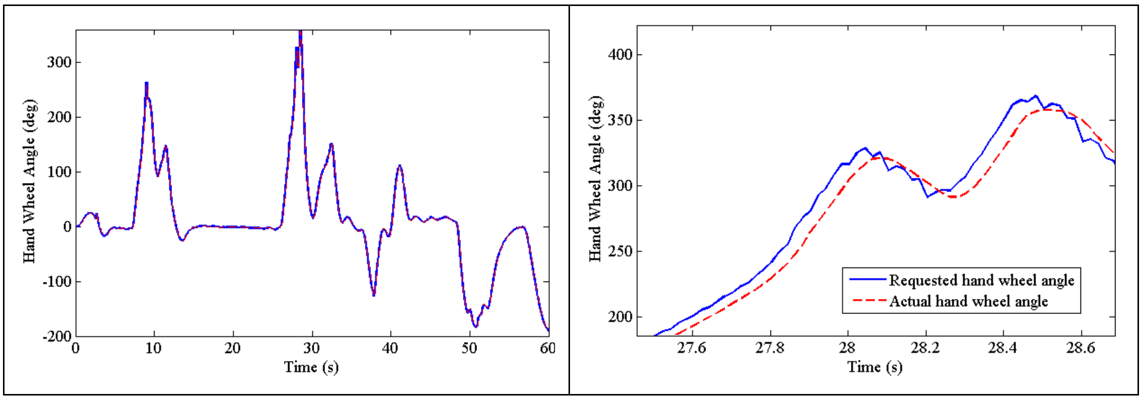

Figure 45: Control signal during one lap on the Råda track (left). A close up on the requested hand wheel angle and the actual can be seen to the right. The peaks in steering wheel angle are a result from saturated front wheels giving a rapid increase in requested angle.

8.3 Dependence on tuning

The tuning of the controller used in physical testing is done in simulations with a model of the SAAB 9-5 in CarMaker. The friction was set to a value corresponding to dry tarmac during the calibration and a tire model from CarMaker was used. Despite the model being of a front wheel driven car (a four wheel drive version was used in physical tests) and different sets of tires being used the controller worked well. The controller was also tested during wet conditions with good results.

8.4 Double lane change test

Although the double lane change manoeuvre hasn’t been considered specifically during the development a brief test was made using the standard *Preview Curvature Controller*. During the test the car was equipped with all season tyres. The cones were positioned roughly as the ISO-17387 lane change standard.

The most important result from the lane change test is that the controller proved to execute very repetitive and precise control. The maximum possible entry speed was 65 km/h limited by the rather low performing tyres. Figure 46 shows 13 runs of the lane change with speeds from 45-65 km/h. Although the front tyres partly saturated in the first turn at 65 km/h it can be seen that the repeatability is very good. Once the reference track had been adjusted to achieve a good path through the cones the controller drove the same path regardless to speed up to the limit.

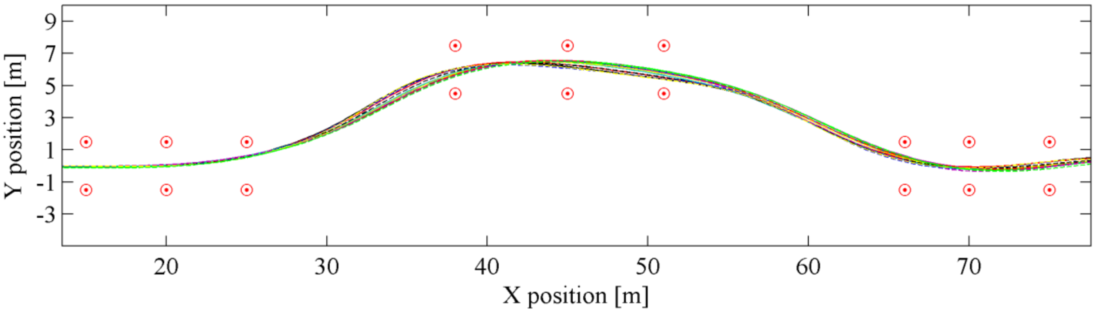

Figure 46. Lane change test. The figure shows 13 runs with speeds from 45-65 km/h. As seen the repeatability is very high.

9 Discussion

The developed *Preview Curvature Controller* does show very good performance and definitely fulfils the aims and demands of the thesis. As discussed briefly in chapter 7.1.2 the controller will not give absolute precision, due to the corner cutting. However, since it is developed for driving at a track with margins on either side it is of little disadvantage that there is a deviation of up to 1.5 meters. As long as the tires are not saturated 1.5 meters has been the largest error observed during testing.

Instead of absolute precision, repeatability is the most important performance criterion of the controller. The repeatability is a necessity for comparing different settings of for example suspension and ESP parameters.

To improve the absolute precision of the controller the desired path sent to the controller could be compensated for the corner cutting. As the corner cutting is a result of the preview distance which is dependant of the speed, it is necessary to know the approximate speed when entering the corner to compensate for the corner cutting.

If the front tyres saturate there is a risk that the controller requests a steering value considerably higher than the angle giving maximum lateral acceleration at the current speed. To request a steering angle close to this peak in such conditions a moving threshold value for the steering angle could be added to the controller. The threshold value would be decreasing with increasing speed.

The potential of the controller was also shown to be very high as it was possible to perform a double lane change at almost as high speed as an experienced test driver, could perform it (65 km/h) after only 30 minutes of adjusting the reference track. The speed itself is not what is most impressive, but rather that the same path was followed in all test runs.

Inspiration to the controller has come partly from the layered models studied in chapter 3 where state feedback is given to stabilize the vehicle. It was however found more effective to combine the layers by using the attitude angle, rather than heading, to calculate the preview point. By using the attitude angle the controller will try to align the car automatically if a sudden and unwanted yaw motion occurs.

9.1 Comparing simulations with physical testing

The results from physical testing agree very well with the simulation results. The corner cutting driving behaviour is similar and the lateral error is also very similar. In order to improve the quality of comparison it would be beneficial to have equal longitudinal control. As IPG-driver has performed longitudinal control in the simulations while human test drivers has actuated the brake and throttle in the physical testing an exact comparison between simulations and physical testing has not been performed.

Something that is difficult to evaluate in simulations is how smooth a human perceives the controller. However, steering wheel angle velocity and acceleration were studied to avoid too high values. The physical testing confirmed that the developed controller performs smooth actuation and the perceived safety is good.

9.2 Future work

The developed controller does have very good performance and would be ready for use as designed. However, before commercialization it would be necessary to add more safety functions for system failures etc. Additionally, there was not enough time to implement and perform physical testing of the *Control of Specific Manoeuvres* described in chapter 0. Furthermore, the coupling with a longitudinal vehicle controller and use of other measurement systems is necessary to study in order to commercialize the controller.

9.2.1 Coupling with longitudinal control

An obvious extension of the lateral vehicle controller presented in this thesis is to couple it with longitudinal control. A longitudinal controller would demand pedal actuators or similar in order to be implemented. A suitable system for actuation is available from Vehico Gmbh, along with a controller with a desired speed as reference signal.

As the *Preview Curvature Controller* was developed decoupled from the longitudinal controller and has proven to work well even when having high longitudinal accelerations the coupling between the two controllers can be kept rather limited and still achieve a good performance. A proposed solution is to include a desired speed in the `DriveStraightLine` and `DriveCurve` commands. A way of decreasing the number of parameters that the user would have to input is to set a limit to the maximum allowed lateral acceleration and have the controller calculate the appropriate speed in each segment of the track.

Another connection between the controllers that would increase the performance is a limit to acceleration dependant of steering wheel angle, so that the controller does not try to accelerate too violently out of a corner. This was experienced to be a problem when IPG driver was controlling the speed of the vehicle, as it was completely decoupled from the lateral controller.

9.2.2 Using other measurement systems

The choice of measurement systems to be used in the thesis was made considering what was available at SAAB. Therefore we had no access to a combined GPS and IMU or an RTK system. The use of a combined inertial and GPS navigation system would remove the need of the Kalman filter that has been used during the physical testing. An RTK system would increase the absolute accuracy of the system, but would increase the demands on the facility used as a calibrated base station must be available.

Most GPS and IMU systems should be compatible with the controller if they can communicate over a CAN bus. To achieve the same performance as presented in this thesis a low drift gyro should be used, but the drift could also be compensated for by adapting the yaw angle to the GPS heading angle when the lateral acceleration is close to zero. The demand on the GPS is primarily that it should provide a 100 Hz position signal.

9.2.3 Creation of tracks

Creating a reference track relative to a physical track to be followed showed to be a rather time consuming task during the thesis. The task was performed by using an aerial photo of the track and then measuring the radius and degrees of the turns and the length of the straights. To make this task more time efficient either an automated way of creating a track from a picture or a function to rerun a manually driven track should be implemented.

9.3 Sustainable development

The main contribution the robot controller has to a sustainable development is to improve the effectiveness in chassis development. This will help any company who uses the robot to develop competitive products that is attractive to the customers, while still having a cost effective organization.

The controller presented in this thesis could also be further developed to use inputs from vehicle mounted cameras and radar systems. This could enable totally autonomous vehicles. By communication between these autonomous vehicles and the current traffic situation these vehicles can cooperate to improve traffic safety and traffic flow, leading to more effective transportation.

10 Conclusions

The controller developed during this thesis uses a new method of feedback path control which continuously changes the reference signal based upon vehicle location. The controller calculates the curvature required to arrive at a preview point on a predefined track ahead of the vehicle. Compared to the related steering controllers found in previous research the newly developed controller uses a more straightforward way of calculating controller inputs from track deviation and vehicle states. The controller also uses a simple yet effective way of, given a reference input, calculating the required steering angle using an exponential function.

The absence of multiple controller inputs gives a great advantage since it is easy to analyse and understand why the controller behaves as it does, and how to customize it for specific demands that may differ from the present ones. It is also very easy to calibrate and tune the controller to different cars and tracks.

Despite its relative simplicity and low computational demand the *Preview Curvature Controller* shows very good performance both in simulations and in physical testing. Driving on a narrow track at high speed the deviation from the defined track has been kept below 1.5 meters, but more importantly the repeatability is close to absolute. It has also proven stable for disturbances to input signals and to the vehicle itself. The actuation of the steering has during the testing been perceived to be smooth and the operators has felt confident in the safety of the system.

11 References

B. W. Karl J. Åström (1997): *Computer Controlled Systems*. Prentice Hall, Upper Saddle River.

H. B. Pacejka (2005): *Tire and Vehicle Dynamics*. SAE International,

Wikipedia (2011): *Global Positioning System*. 2011-05-23.

Wikipedia (2011): *Inertial Navigation Systems*. 2011-05-23.

IPG Automotive GmbH (2011)

E. Donges (1978): *A two-level model of driver steering behaviour*. *Human factors*, 20, 6, 691-707.

J. Edelmann, M. Plöchl, W. Reinalter and W. Tieber (2007): *A passenger car driver model for higher lateral accelerations*. *Vehicle System Dynamics*, 45, 12, 1117-1129.

P. Falcone, H. Eric Tseng, F. Borrelli, J. Asgari and D. Hrovat (2008): *MPC-based yaw and lateral stabilisation via active front steering and braking*. *Vehicle System Dynamics: International Journal of Vehicle Mechanics and Mobility*, 46, 1 supp 1, 611 - 628.

D. P. Kelly and R. S. Sharp (2010): *Time-optimal control of the race car: a numerical method to emulate the ideal driver*. *Vehicle System Dynamics*, 48, 12, 1461-1474.

M. Kondo (1953): *Directional stability (when steering is added)*. *Journal of the Society of Automotive Engineers of Japan (JSAE)*, 7, 5-6.

Y. Lin, P. Tang, W. J. Zhang and Q. Yu (2005): *Artificial neural network modelling of driver handling behaviour in a driver±vehicle±environment system*. *International Journal of Vehicle Design*, 37, 1,

M. Plöchl and J. Edelmann (2007): *Driver Models in Automobile Dynamics Application*. *Vehicle System Dynamics,* 45, 699-741.

M. Plöchl and P. Lugner (1999): *A3-level driver model and its application to driving simulation*. *Vehicle System Dynamics Supplement*, 33, 71-82.

L. D. Reid (1983): *A survey of recent driver steering behavior models suited to accident studies*. *Accident Analysis and Prevention*, 15, 1, 23-40.

R. S. Sharp, D. Casanova and P. Symonds (2000): *A Mathematical Model for Driver Steering Control, with Design, Tuning and Performance Results*. *Vehicle System Dynamics: International Journal of Vehicle Mechanics and Mobility*, 33, 5, 289 - 326.

H. E. Tseng, J. Asgari, D. Hrovat, P. van der Jagt, A. Cherry and S. Neads (2005): *Evasive manoeuvres with a steering robot*. *Vehicle System Dynamics*, 43, 3, 199-216.

G. Xi and Y. Qun (1994): *Driver-vehicle-environment closed-loop simulation of handling and stability using fuzzy control theory*. *Vehicle System Dynamics Supplement*, 23, 172-183.

iMAR_GmbH (2006): *iDIS-FMS Product Summary*.

Race_Logic (2009): *VBOX III 100Hz GPS Data Logger User Guide*.

B. Schmidtbauer (2010): *TME 165 Measurement Techniques for Automotive Applications - Signals and Systems, Lecture Notes*.

D. Casanova (2001): *On minimum time vehicle manoeuvring: The theoretical optimal lap*. PhD. Cranfield University, Cranfield,

Race_Logic (2011): http://www.velocitybox.co.uk/index.php/en/products-main/37-gps-accuracy.html -

Vehico (2011): http://www.vehico.de/ - 2011 April 27.